

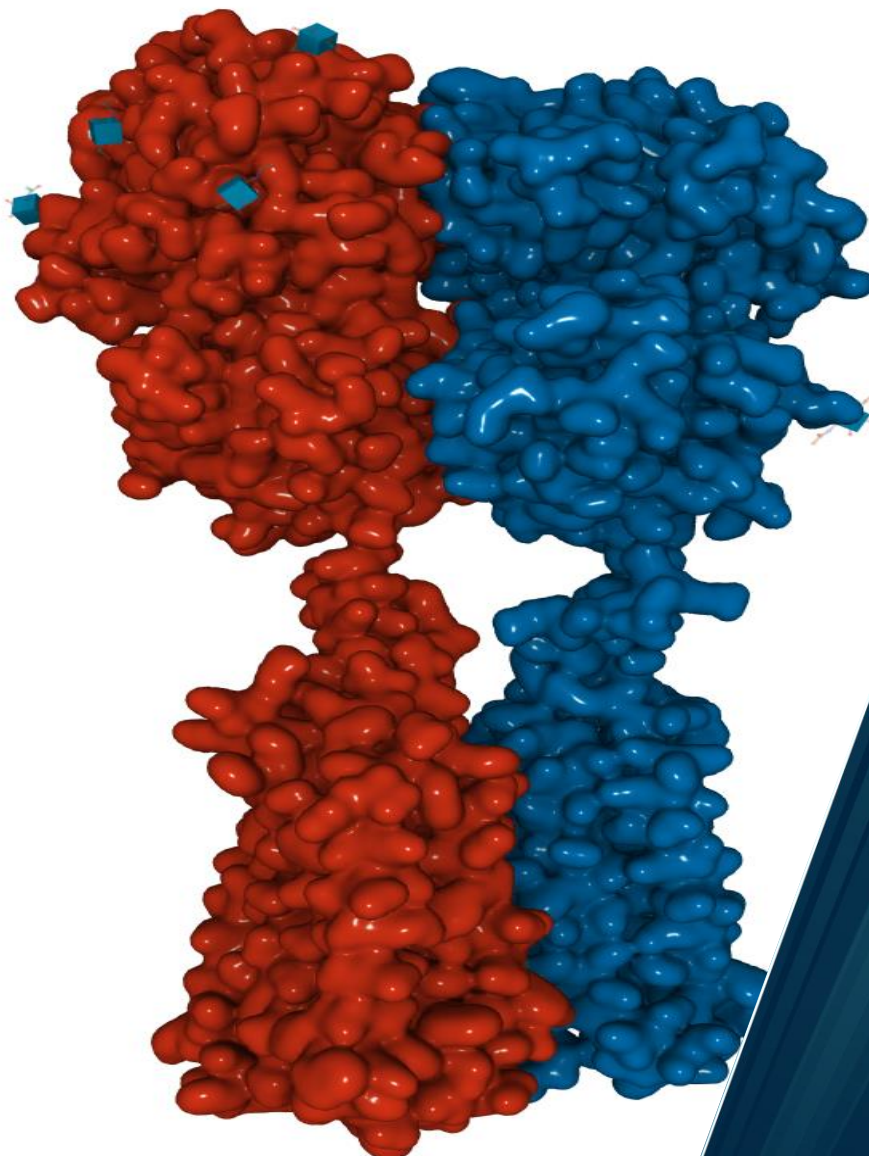


Faculty of Health Sciences, Department of Medical Biology, Molecular Pharmacology and Toxicology Research Group

Improving and utilizing functional in vitro cAMP assay in pursuit to discover allosteric modulators of the GABA_B receptor

Torkild Pettersen

Master's thesis in Biomedicine (MBI-3911) July 2021



Cover image: PDB article 7C7Q, metabotropic GABA type B receptor. Edited to preferred esthetic using PDB's own edit interface.

Acknowledgments

This study and master thesis serves as the conclusion for my master in Biomedicine at the University of Tromsø – The Arctic University of Norway. The project was conducted with and as a part of the Medical Pharmacology and Toxicology research group at the Institute of Medical Biology (IMB), Faculty of Health Sciences. The work was conducted from August 2020 to July 2021.

It has been a great honor to be a part of this project. And I would like to express my utmost gratitude to both my supervisor Professor Ingebrigt Sylte and co-supervisor Chief Engineer Imin Wushur, for teaching and guiding me through this project. And especially for accompanying me while working long nights in the lab. I cannot imagine where I would be without the two of you. I hope that I get to work with both of you in the future.

I would also like to extend my gratitude to my fellow master students that I've shared office with during the course of conducting research and writing the thesis, especially my good friend Aumkar Logendran, for making the thesis writing ever so joyful. It has been amazing to be a part of the master course because of you guys!

Last, but not least, I would like to extend my gratitude to HelseNord for their support with funding the project under project number HNF1426-18, and our collaborators from Poland professor Andrzej j. Bojarski and his research group at the Polish Academy of Sciences for synthesizing the compound hits investigated in my thesis.

Abstract

The GABAergic system is the main inhibitory neuronal system utilized within the central nervous system (CNS). γ -aminobutyric acid (GABA) is the fundamental neurotransmitter which transmit inhibitory signals through GABA receptors, the ionotropic GABA_A and GABA_C receptors; and the metabotropic G-protein coupled receptor GABA_B receptor. Disruption of this system is associated with a range of psychiatric disorders such as depression, anxiety, addiction, and schizophrenia, among others. The efficacy of common antidepressants is dependent on their ability to restore conventional GABAergic function.

As of 2021, the agonist baclofen is currently the only approved clinical drug targeting the metabotropic GABA_B receptor. However, due to its limitations it was not originally applicable for use on receptors within the brain. A large magnitude of GABA and baclofen analogues have been discovered, though none have shown promise for application towards clinical use within the brain *in vivo*. Which has led to the investigation of allosteric modulation of the receptor.

In the present study, *in vitro* cAMP accumulation assay and radioligand binding assay were used in combination to thoroughly test compounds discovered through virtual screening in pursuit to discover pharmacologically active allosteric modulators. Several compounds were found to increase or decrease effects of GABA, RB-490 and TI400 were the most promising candidates.

Table of Contents

Acknowledgments	i
Abstract	ii
Abbreviations	v
1 Introduction	1
1.1 The central nervous system (CNS).....	1
1.1.1 Signal generation: The Action Potential	2
1.2 G-protein coupled receptors (GPCRs) and G-proteins.....	5
1.2.1 Family C receptors	8
1.3 The GABAergic system.....	9
1.3.1 GABA _B receptor.....	10
1.3.2 GABA _B receptors outside of the CNS.....	13
1.3.3 GABA _B receptor compounds	14
1.4 Blood-brain barrier and drug distribution to CNS.....	16
1.5 Allosteric modulation	16
1.5.1 Agonist- and antagonist-like allosteric binders	18
1.6 In Vitro methods.....	19
1.6.1 Cell culturing.....	19
1.6.2 Chinese Hamster Ovarian (CHO) cells	20
1.6.3 cAMP accumulation assay	20
1.6.4 Radioligand-binding assay	22
2 Aim.....	23
3 Material and Methods.....	24
3.1 Cell culturing	26
3.2 cAMP accumulation assay.....	27
3.2.1 Prerequisite factor-dependent assay	30

3.3	Optimization	31
3.4	Radioligand binding assay	31
4	Results	34
4.1	Method	34
4.2	cAMP accumulation assay	34
4.2.1	Wild-type assay	36
4.2.2	Compound dose-response	37
5	Discussion	38
5.1	Optimization	38
5.2	Compound test	39
6	Conclusion	42
7	Further prospects	42
8	References	43
9	Appendices	52
9.1	Appendix A	52
	Cell culture and assay recipes	52
9.2	Appendix B	53
	Test compounds from the Polish Academy of Sciences	53

Abbreviations

7TM	Seven Transmembrane Domain
AC	Adenylyl Cyclase
ago-NAM	Agonist-like Negative Allosteric Modulator
ago-PAM	Agonist-like Positive Allosteric Modulator
ATP	Adenosine Triphosphate
BBB	Blood-Brain Barrier
Ca²⁺	Calcium
cAMP	Cyclic-Adenosine Monophosphate
CHO	Chinese Hamster Ovarian cells
Cl⁻	Chloride
CNS	Central Nervous System
CRD	Cysteine Rich Domain
CRE	cAMP Response Element
CREB	cAMP Response Element Binding protein
DAG	Diacylglycerol
DG44 CHO	DHFR ^{-/-} modified CHO
DHFR	Dihydrofolate Reductase
DMSO	Dimethyl Sulfoxide
EA	Enzyme Acceptor
EC₂₀	Effective Concentration for 20% stimulation
EC₈₀	Effective Concentration for 80% stimulation
EC₁₀₀	Effective Concentration for max stimulation
ED	Enzyme Donor
FAK	Focal Adhesion Kinase
GABA	γ -Aminobutyric Acid
GABA_A	γ -Aminobutyric Acid A Receptor
GABA_B-R	γ -Aminobutyric Acid B Receptor
GABA_C	γ -Aminobutyric Acid C Receptor
GDP	Guanosine Diphosphate
GF	GABA-Forskolin mixture
GFC	GABA-Forskolin-Compound mixture
GIRK	G-Protein-Gated Inward Rectifying K ⁺ channel
GMO	Genetically Modified Organism
GPCR	G-Protein Coupled Receptor
G-protein	Guanine Nucleotide-Binding Protein
GRAFS	Glutamate-Rhodopsin-Adhesion-Frizzle-Secretin System
GRK	G-Protein Coupled Receptor Kinase
GTP	Guanosine Triphosphate
HBSS	Hank's Buffered Saline Solution
¹²⁵I	Iodine 125
IP3	Inositol Triphosphate
K⁺	Potassium
MAP	Mitogen Activated Protein kinase
mGlu	Metabotropic Glutamate Receptor

mRNA	Messenger Ribonucleic Acid
Na⁺	Sodium
NAM	Negative Allosteric Modifier
PAM	Positive Allosteric Modifier
PAM- antagonist	Antagonist-like Positive Allosteric Modifier
PBS	Phosphate Buffered Saline
PLC-β	Phospholipase C-β
PIP₂	Phosphatidylinositol-4,5-bisphosphate
PKA	Protein Kinase A
PKC	Protein Kinase C
RhoGEF	RasATPase Nucleotide Exchange Factor
RLU	Relative Light Unit
ROCK	Rho-associated protein Kinase
SAM	Silent Allosteric Modifier
SRF	Serum Response Transcription Factor
VFD	Venus Flytrap Domain
VGCC	Voltage-Gated Calcium Channel

1 Introduction

1.1 The central nervous system (CNS)

The central nervous system (CNS) is a highly complex and sophisticated organ in charge of receiving, storing, and processing sensory inputs and initiating corresponding motor functions and/or more complex emotional patterns and thought processes (1). The brain is divided into four main anatomical parts: the cerebral hemispheres, which include the cortex, basal ganglia and hippocampi among others; diencephalon, including the hypothalamus and thalamus; brain stem, comprising of the midbrain, pons and medulla; and the cerebellum (1,2). In addition to the brain, the CNS also includes the spinal cord, however it won't be explored further as the present thesis focuses on the brain-portion of the CNS.

The main roles of the nervous system are receiving sensory signals, communicating signals to specific regions for processing, processing the signals and commencing the signal response. These functions are summarized into, sensation, integration, and response (3,4). The brain stem provides sensory information from the head and neck area, and lead tracts from the spinal cord to the brain to provide the brain with information from the periphery. The brain stem consists of; the midbrain, in charge of eye movements and the transport of information from the eyes to the brain; the pons, which leads the signalling tracts between the cerebrum and cerebellum, and from the body to the thalamus; and the medulla, which contains the autonomic centres in charge of regulating heart rate, breathing and blood pressure. Lastly the cerebellum, which is important for planning and smooth execution of movements, and maintaining posture (1,3–5).

These structures comprise of a complex orientation and sequences of nerve- and glial cells. The nerve cells, or neurons, are the primary cell type of the nervous system and are responsible for relaying signals after a sensory input (3,4). Neurons consist of three main parts; the cell body, the soma; the myelinated axon; and the axon terminal, all depicted in **figure 1**. The soma has branching dendrites increasing its surface area, such that the neuron reaches and connects with axon terminals of other neurons. These connections are called synapses or synaptic clefts. Functionally the soma senses and receives stimuli, or rather information, and generates an action potential downstream. Downstream from the soma is the axon, which is an elongated part of the neuron, providing the neuron the majority of its length. The axon itself is myelinated; meaning that segments of myelin sheaths are wrapped around the soma, to insulate the axon and isolate it from the extracellular matrix which could interfere with the signal. Lastly the axon terminal, which is essential for relaying the signal, the information, to the following

neuron (1,3–5). In some cases, like the motor neurons of the muscle and the neurons in posterior pituitary gland, the axon terminals do not terminate in other neurons (3,4).

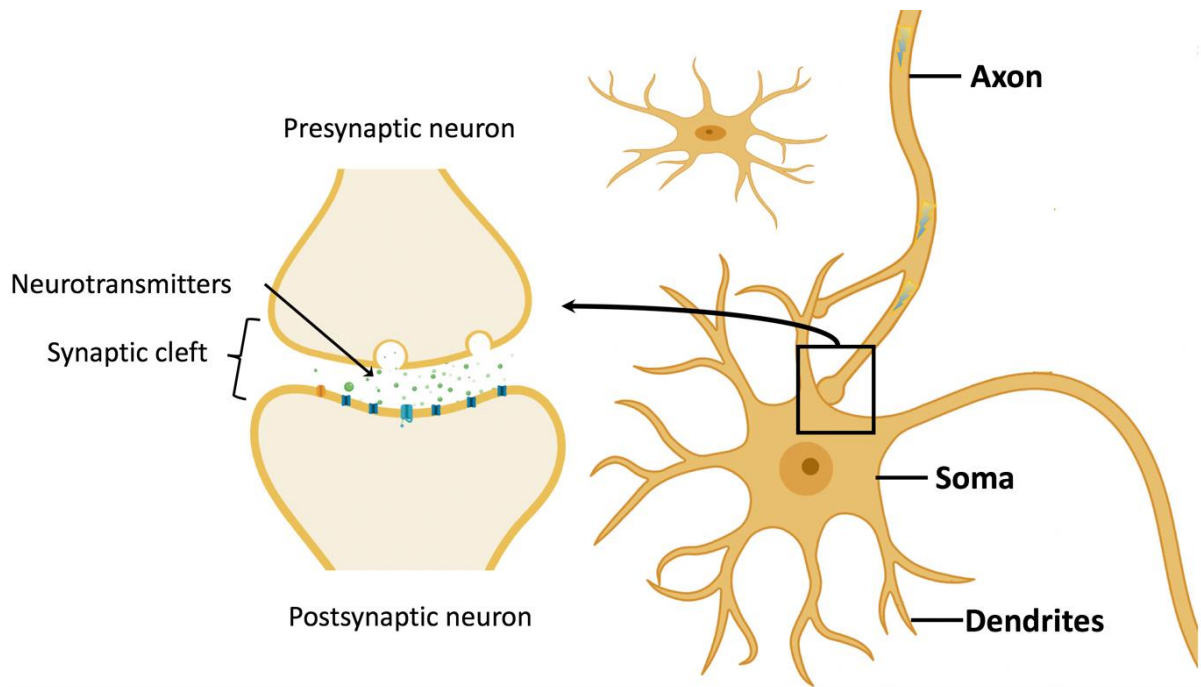


Figure 1: Illustration of the major cellular structures which constructs a neuron. The neuron is a complex elongated cell consisting off a soma, myelinated axon and an axon terminal. The soma contains branching dendrites which stretches out to cover a larger surface area and make connections with another neuron's axon terminals to form synaptic clefts. The elongated axon provides the neuron length and carries the signal downstream towards the axon terminal. Myelin sheets wrap around the axon to create an insulating barrier to the extracellular space, protecting the electrochemical signal. This signal causes neurotransmitters to be released from the axon terminal to the target cell or tissue. Figure adopted from (6,7).

1.1.1 Signal generation: The Action Potential

The transmission of signals via neurons has both a chemical and an electrical aspect. The major components involved in generating the signals are ions and ion channels, and in order to simplify the explanation of the relationship between these and the neuron action potential; we can divide the generation into three membrane potentials, the resting-, activating- and inactivating potential (3). The ion balance between the outside of the neuron, the extracellular matrix, and the inside of the neuron creates a membrane potential, which is the collection of electrochemical forces exerted upon the membrane. The resting potential is the natural potential that the neuron membrane will have when the neuron is not excited or recovering from a previous excitement (8). Importantly, there is a difference in ion concentrations between the inside and outside of the neuron. Specifically, the concentration of sodium (Na^+) and potassium (K^+) ions. The concentration of Na^+ is higher on the outside than on the inside, while K^+ is

higher on the inside than on the outside. This is due to the important Na^+/K^+ -ATPase, which utilizes chemical energy in form of adenosine triphosphate (ATP) to pump Na^+ and K^+ against their concentration gradients (3,8). Thus, creating a chemical force upon the membrane. Each ion has an equilibrium potential, this is the potential when there is no net flow of ions across the membrane. In physiological conditions the equilibrium potential for Na^+ and K^+ is +55mV and -103mV respectively (8). Lastly, since K^+ dominates transport into the cell, the overall equilibrium potential is closer to the K^+ equilibrium potential than that of Na^+ . In standard physiological conditions the equilibrium potential is approximately -60 mV, creating the electrical potential (3,8).

The electrochemical forces that are put onto Na^+ are essential for a signal generation. Since both the chemical and electrical forces favours the influx of Na^+ into the neuron, the influx happens rapidly when facilitated. The last important part for creating the signal is the initial stimulus (3,8). Neurons can utilize different sets of sensory receptors to sense a stress stimulus in their environment, some examples are: thermoreceptors, both hot and cold sensing; chemoreceptors, chemical stimuli like taste and smell; mechanoreceptors, for mechanical stimuli like touch and vibration. There are also more specialized receptors like the baroreceptor, photoreceptor, proprioceptors and osmoreceptors, all of which have essential roles within the human body (3). Classical neurons which are stimulated by pre-synaptic neurons, a neuron stimulated by a neuron, can start the flow of Na^+ through ligand-gated ion channels. Ion channels that open when bound by neurotransmitters, is facilitating the influx of Na^+ and the depolarisation begins. Once the influx of Na^+ starts, the membrane obtains a new equilibrium potential that it will try to reach. When the membrane potential reaches -50 to -55 mV, the threshold potential is reached. The threshold potential is categorized by the sudden increase in depolarizing rate beyond the threshold. Which happens due to a specialized voltage-gated ion channel, an ion channel that is sensitive to a specific voltage and opens for ion flux once that voltage is reached (3,8). The channel allows the membrane potential to reach upwards to +40 mV, as illustrated in **figure 2**. This membrane potential is levelled across a larger region of the membrane, causing nearby voltage-gated ion channels to reach their threshold. This sequence of events continues downstream the neuron, via the axon, until it reaches the axon terminal. At the terminal, voltage-gated ion channels permeable to calcium (Ca^{2+}) are reached and influx of Ca^{2+} is facilitated. Ca^{2+} is essential for releasing of neurotransmitters at the axon terminal, causing the signal to be transmitted onto target cells (3,8).

Action Potential Diagram

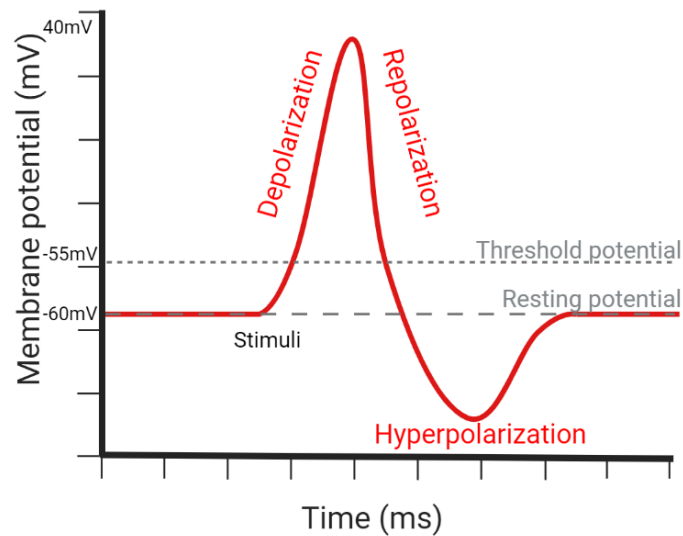


Figure 2: Action potential diagram depicting the electrical membrane potentials during the different phases of an action potential. Created with [Biorender.com](https://www.biorender.com).

1.1.2 Neurotransmitters and neuronal regulation

As previously noted, the neuron is the primary signalling unit in the nervous system which sense, conduct, and transmit electrochemical signals through depolarizations called action potentials, and transmit the signal utilizing synaptic clefts. There are two main types of synapses, electrical and chemical, in which electrical does not utilize neurotransmitters and directly share ions with connected neuron through cellular junctions such as gap junctions (1,3). Electrical synapses, however, have a larger synaptic cleft composing of extracellular matrix molecules, where the presynaptic neuron facing its axon terminal towards the synapse releases neurotransmitters into the cleft to interact with the postsynaptic neurons receptors, which can be located on the soma, axon, axon terminal, and neuron spines (3). The receptors can either be ionotropic like the nicotine acetylcholine receptors and the serotonin 5-hydroxy tryptamine 3 receptor, or metabotropic receptors also named guanine nucleotide-binding protein (G-protein) coupled receptors, like the glutamate receptor. Ionotropic receptors act as ligand-gated ion channels, which upon neurotransmitter binding open and allow the influx of selected ions to either depolarize or hyperpolarize the postsynaptic neuron. Metabotropic receptors mediate a cellular signal through a signal cascade and creating second messengers (1,3,8).

1.2 G-protein coupled receptors (GPCRs) and G-proteins

G-Protein Coupled Receptors (GPCRs) is the largest protein superfamily across mammalian genomes and can be divided into six major classes, or families, and hundreds of subfamilies (9). The six classes are: the rhodopsin-like, class A; the secretin-like, class B; the glutamate receptor-like, class C; the fungal pheromone receptors, class D; the fungal cyclic adenosine monophosphate (cAMP) receptors, class E; and the opsin receptors of invertebrates, class F (10). Evidentially, humans do not possess classes D-F and are therefore restricted to the first three, classes A-C (10). With all these classes, and more importantly those found in mammals, there is no significant sequence similarity between them (9–11). However, the GPCR classes still share structure and function similarities (9). Namely they have heptahelical transmembrane (7TM) domains, are associated with cell signalling through G-proteins in a large variety of cellular processes, and different variations can receive stimuli from hormones, neurotransmitters, ions, photons, and other sources (11).

Following the GRAFS system there is five main classes which together comprise the GRAFS acronym, these being Glutamate-like, Rhodopsin-like, Adhesion-like, Frizzles/Taste2 and Secretin-like (10). Fortunately, this system goes hand-in-hand with the aforementioned classes, describing class A (rhodopsin-like), class B (secretin-like and adhesion-like), class C (glutamate-like) and class F (frizzles/taste2) (10). Structures of representative GPCRs belonging to the different GRAFS system classes, and their conformational change upon activation are shown in **figure 3**. The major difference being the extracellular loop regions, emphasizing the specificity of the different families; and sequence differences in the transmembrane regions that supports the arrangement differences of extracellular loops (9). The differences within a class create a large repertoire of receptors in each subfamily. Class A being the largest with close to 700 unique human receptors (11).

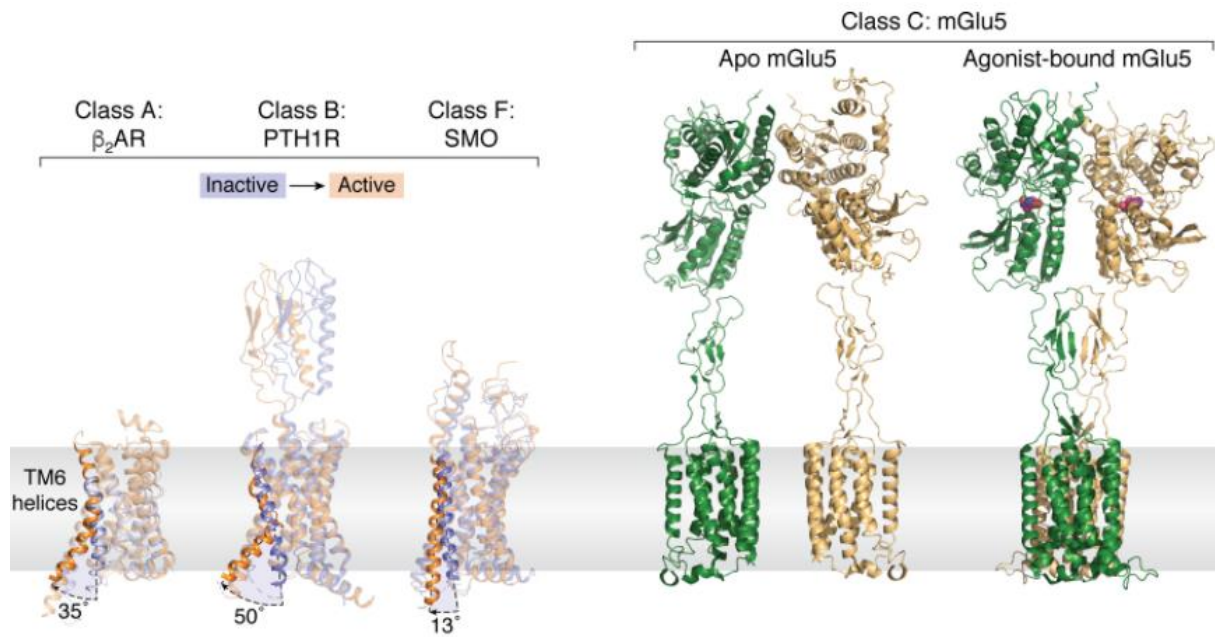


Figure 3: Illustrating the structure of representative GPCR classes and the conformational change when bound to agonists using superimposed structures from the PDB database ([RCSB PDB: Homepage](https://www.rcsb.org/)). Classes A, B, and F share the conformational change being the outward bend of transmembrane helix nr.6 shown in orange, emphasized by greying out the remaining parts of the receptor. Class C with its vastly different structure and heterodimeric complex differs from the other classes, moving together and entangling the transmembrane domains. Figure adopted from (12).

The main mode of action is relaying signals through G-proteins. G-proteins are heterotrimeric proteins, meaning they consist of three unique subunits: $G\alpha$, $G\beta$, and $G\gamma$. There are also multiple variations of G-protein subunits with different signalling bias, currently known there are: 20 $G\alpha$, 6 $G\beta$, and 11 $G\gamma$ (13). The $G\alpha$ -proteins can be grouped into four main families based on sequence homology and signalling pathways, these are the $G\alpha_{q/11}$, $G\alpha_{i/o}$, $G\alpha_s$, and $G\alpha_{12/13}$ (13); which respectively utilizes the G_q , G_i , G_s , and $G_{12/13}$ signalling pathways. The $G\alpha$ subunit has a guanosine diphosphate (GDP) bound to it in the inactive trimeric complex. Upon activation of the GPCR, the intrinsic GDP of the $G\alpha$ is swapped for a guanosine triphosphate (GTP); activating the $G\alpha$ causing it to dissociate from the $G\beta\gamma$ complex and travel along the cell membrane to its signalling target. The $G\beta\gamma$ dimer complex has also been found to have signalling significance. The cycle concludes by the hydrolysis of GTP recreating the GDP, inactivating the $G\alpha$ and terminating the signalling completely when the $G\alpha$ reassociates with the $G\beta\gamma$ complex into the trimeric complex (14,15).

G_q pathway G-protein have one main destination, being the activation of phospholipase C- β (PLC- β). The PLC- β continues the pathway by cleaving the membrane component phosphatidylinositol 4,5-bisphosphate into free inositol triphosphate (IP3) and anchored diacylglycerol (DAG) (16). IP3 releases calcium from intracellular storages, which bind

calcium dependent calcium-channels allowing more extracellular calcium to flux into the cell. While DAG recruits and activates protein kinase C (PKC) (13). $G_{\alpha_{i/o}}$ signals through the $G_{i/o}$ pathway which is known for inhibiting the adenylate cyclase (AC) and is utilized by essential hormones and neurotransmitters (13,16). The associated $G\beta\gamma$ complex also signal through this pathway by regulating specific isoforms of effector proteins such as the PLC- β , K^+ -channels, phosphatidylinositol 3-kinase, proteins of the Ras superfamily indirectly, and similarly to G_{α} the AC (13,16). Conversely the G_{α_s} , utilizing the G_s pathway, stimulates AC into converting more cAMP which can mediate a variety of effects through the cAMP dependent protein kinase A (PKA); including, but not limited to, the mitogen-activated protein kinase (MAP kinase) pathway, phosphorylase kinase for metabolism, and gene expression (13). Lastly the $G_{12/13}$ family pathway, which despite being grouped together the $G_{\alpha_{12}}$ and $G_{\alpha_{13}}$ have different signalling connections (13). Thereby creating a unique G_{12} and G_{13} pathway. $G_{\alpha_{12}}$ is the least established of the two, having only shown connections to different proteins without knowing the mechanism or full pathway; $G_{\alpha_{12}}$ interacts with tyrosine kinases, cadherins, catenins, the GTPase RasGAP, and permease Gap1 (16). While $G_{\alpha_{13}}$ stimulates RhoGTPase nucleotide exchange factor (RhoGEF) which downstream activates the RhoA GTPase. RhoA interacts with multiple less studied effector molecules, and with more studied Rho kinases known as ROCKs. ROCK activation leads to focal adhesion kinase (FAK) activation through phosphorylation, with an endpoint being the serum response transcription factor (SRF) mediating gene expression (13,16,17).

Upon ligand binding, activation and signal transduction using G-proteins, the GPCR will also become susceptible to phosphorylation through a G-protein independent pathway conducted by G-protein-coupled receptor kinases (GRK) (15). The phosphorylation of the receptor marks it for arrestin binding which competitively covers and masks the G-protein interaction site of the GPCR, effectively desensitizing the receptor (18). The arrestin partners are the clathrins and the clathrin adaptor AP2 mediating cellular trafficking of bound proteins, in this case internalizing the GPCR. Internalized GPCR can be recycled back to the membrane or through ubiquitination be sent to degradation in lysosomes (15,18). However, ubiquitinated receptor-arrestin complex can also be deubiquitinated and recycled back to the membrane (18), although how this choice is made is still poorly understood.

1.2.1 Family C receptors

Class C, or rather family C, GPCRs as shown in **figure 3**, are differentiated from other GPCRs by their large extracellular region called the Venus flytrap domain (VFD), due to the uncanny similarity to the Venus flytrap plant, a cysteine rich domain (CRD) bridging the VFD and 7TM, and obligate dimerization between the two subunits for activation (19). Similarly, to family A receptors, the family C GPCRs also exists in an equilibrium of active and inactive states, with agonists and antagonists shifting this equilibrium in either direction respectively (14). Contrary to other families, with orthosteric sites in the 7TM domain (19), the family C orthosteric site is located on the characteristic VFD portion of the receptor. Upon ligand binding the receptor VFDs dimerize and effectively cause a downstream conformational change and receptor activation (14). The CRD portion of the receptor is a longer amino acid chain with nine highly conserved cysteines that link the VFD to the 7TM (20). Studying the metabotropic glutamate receptors (mGlu) that belong to the family C, the CRD was found to be essential for receptor activation (21). The 7TM domain is a well conserved region among GPCRs due to the orthosteric site which is located on its extracellular portion. However, as previously noted, the family C receptors are the exception, as their orthosteric site is located on the VFD which connects to the 7TM domain (19). The 7TM of family C GPCRs have no significant sequence similarity with other families, however, they are structurally similar. The family C 7TM possess the similar intracellular and extracellular loop regions between the helices, which even give rise to the same crevice that is commonly the orthosteric site in opposed families (14,20,21).

1.3 The GABAergic system

The GABAergic system is the functional structures that uses and utilizes γ -aminobutyric acid (GABA) in their processes. Biosynthesis, release, modulation, effect, and degradation of GABA are all parts of the GABAergic system, as displayed in **figure 4**. This is the main system that mediates inhibitory signals in the CNS, its counterpart is the structurally similar glutamate system which mediates stimulatory signals (22). GABA is an amino acid and is synthesised from glutamate, catalysed by the glutamate carboxylase which removes the carboxyl group from the amino acid backbone of glutamate. And as mentioned prior, GABA's main role is binding to GABA receptors GABA_A, GABA_B, and GABA_C receptors to mediate an inhibitory effect in pre- and/or postsynaptic neurons (22). GABA_A and GABA_C receptors are ionotropic receptors, which are ion channels permeable to chloride ions (Cl⁻); while the GABA_B receptor (GABA_B-R) is a metabotropic family C receptor, a GPCR transducing signals in response to GABA binding (23). Despite sharing an overall function, the GABA_A and GABA_C receptors are significantly different. The GABA_A receptor is a heterooligomer comprising of five subunits with 4TM domains each from a selection of five families (α 1-6, β 1-4, γ 1-4, δ , ϵ , and π), of which the most abundant in the brain is the α 1 β 2 γ 2. The heterooligomer contains two ligand binding sites and a third allosteric site with affinity to benzodiazepines (23). In contrast, the GABA_C receptor comprises of one subunit family, the rho (ρ 1-3) family, and construct either homooligomers or pseudohomooligomer. Of which each of the five subunits have a GABA binding site, making the two receptors functionally different. The GABA_C receptor is more sensitive to ligand binding, less prevalent desensitization, and the channel remain in open confirmation for a prolonged time in comparison to the GABA_A receptor (23).

GABA_B-Rs are generally found distributed throughout the brain, favouring the expression of both receptor subunits simultaneously. Although there are some differences in receptor prevalence and/or prevalence of specific subunits (24). The GABAergic neuron, when stimulated, will release GABA onto postsynaptic neurons; resulting in a inhibitory signal which stop further signal transmission on the postsynaptic end (24).

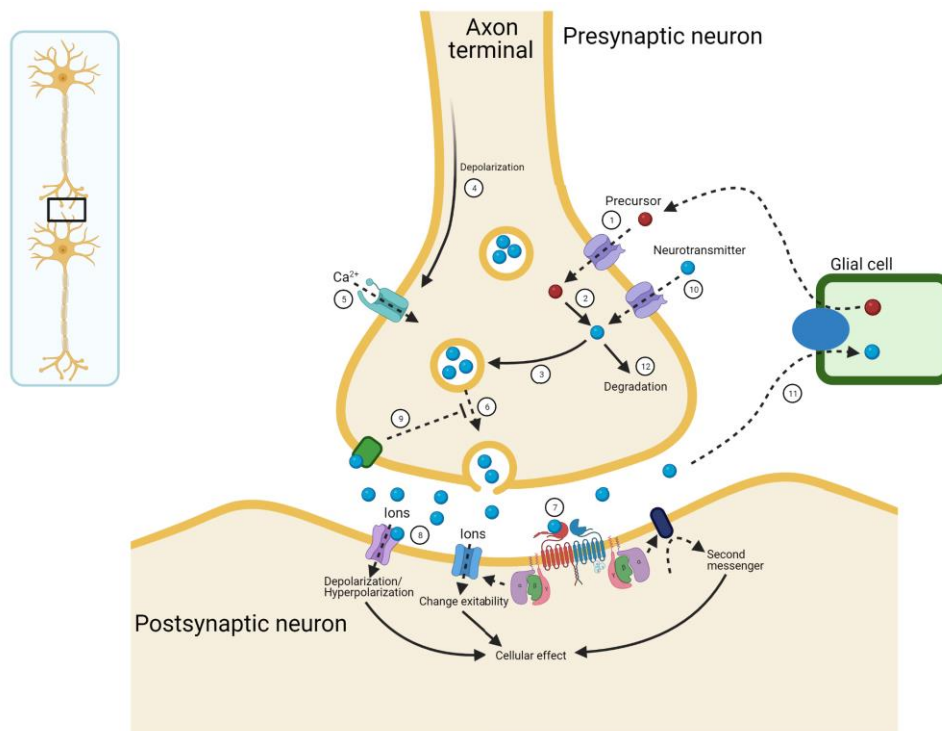


Figure 4: Illustration depicts the function and mode of action of a GABAergic neuron. 1. Neurotransmitter (GABA) precursors (Red) provided by nearby Glial cells are absorbed through protein channels on the presynaptic neuron. 2. Said precursors are biosynthesized into active GABA (blue). 3. Cytosolic GABA are collected and packed into vesicles, primed for exocytosis. 4. Upstream action potential reaches the axon end and causes depolarisation of the axon end. 5. Voltage gated Ca^{2+} -channels open and allow influx of Ca^{2+} . 6. Ca^{2+} allows vesicles to fuse with the plasma membrane and release GABA into the synaptic cleft. 7. GABA binding to receptor causes activation of G-protein pathways ($\text{GABA}_B\text{-R}$). 8. GABA binds directly to ligand-gated channels (GABA_A and GABA_C receptors). 9. GABA bind pre-synaptic receptor to inhibit further release. 10. Reabsorption of GABA directly through protein channels. 11. Absorption of GABA and degradation to precursors by Glial cells. 12. Direct degradation of excess GABA in presynaptic neuron. Created with [BioRender.com](https://www.biorender.com), to accommodate Kantamneni, S. (22).

1.3.1 GABA_B receptor

The $\text{GABA}_B\text{-R}$ is a family C GPCR transducing signals in response to GABA. Unlike its mGlu counterparts the $\text{GABA}_B\text{-R}$ is a heterodimer and does not contain the characteristic CRD (14,19). The heterodimer of $\text{GABA}_B\text{-R}$ consists of the GABA_{B1} and GABA_{B2} subunits, which are structurally similar. The $\text{GABA}_B\text{-R}$ subunits both have the VFD, a 7TM domain and an intracellular tail. However only the B1-unit has an orthosteric site in the VFD (19). But the two subunits are functionally different; the B1-unit is in charge of binding and transmitting signals and the B2-unit stabilizes B1 and aid in modulating the signal transduction (14,19). This is caused by a twisting motion exerted by the B2 lower portion of VFD, the second lobe, upon ligand recognition and dimerization of VFDs, and the coalescence of 7TM domains (14,19). The $\text{GABA}_B\text{-R}$ has been discovered to have two sites, and a potential third, for allosteric binding shown in **figure 5 and 6**. The first and major site is the analogue site for orthosteric

binding in non-family C receptors, being within the 7TM of the B2 subunit between alpha helices TM3, TM5 and TM6. The second site is located between the united subunit's TM6-TM6 interface (25,26). The third site was suggested to be located in the intrahelical domain of the B1 subunit (27). Utilizing a radioligand binding assay and functional assays Porcu and associates confirmed their ligand COR758 to be an allosteric binder and their docking studies revealed a high affinity to the B1 intrahelical domain (27).

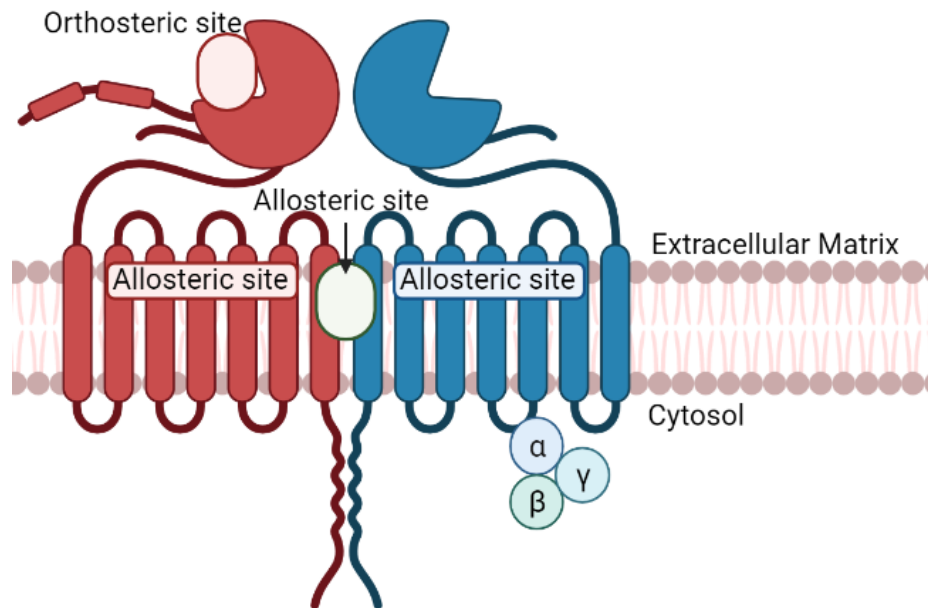


Figure 5: Cartoon representation of GABA_B-R. Illustrates approximate locations of the orthosteric and allosteric binding sites in metabotropic GABA_B-R. The orthosteric binding site is located on the VFD of the B1 subunit (Red), the first allosteric binding site was found in the 7TM domain of the B2 subunit (Blue), a second binding site in the interface between the subunits and a third suggested binding site in the 7TM of the B1 unit. Created with [Biorender.com](https://www.biorender.com).

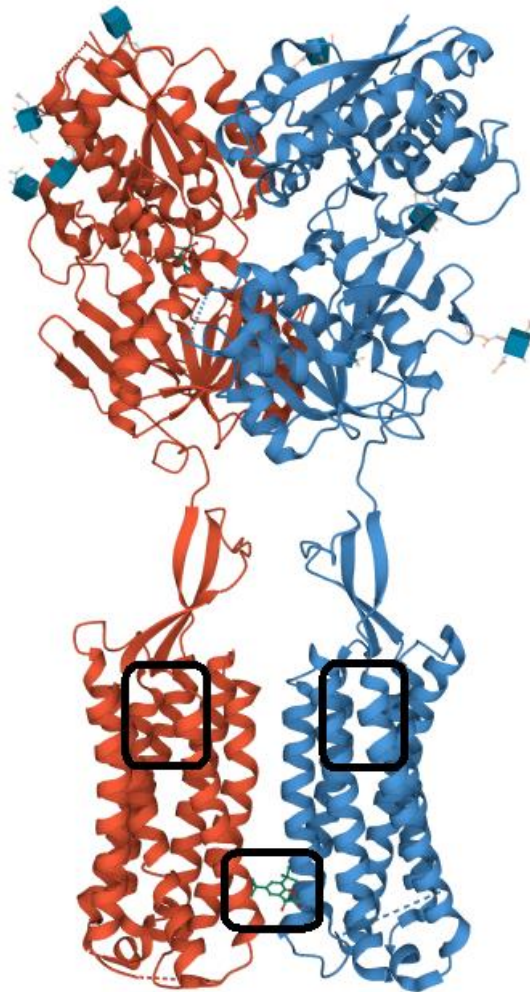


Figure 6: Cryogenic electron microscopy structure of GABAB-R (<https://www.rcsb.org/>; PDB ID: 7C7Q) visualized in ribbons to illustrate allosteric binding sites (Black squares). Between the B1b (Red) and B2 (Blue) subunits, within the TM6-TM6 interface is the third binding site with bound positive allosteric modulator BHFF (R,S-5,7-di-tert-butyl-3-hydroxy-3-trifluoromethyl-3H-benzofuran-2-one).

GABA_B-R interacts with several effector proteins. Mainly the G-protein-gated inwardly rectifying K⁺ (GIRKs) channels, the voltage-gated Ca²⁺ channels (VGCCs) and the AC. GIRK channels are located on the somatodendritic membrane and hyperpolarize postsynaptic neurons through K⁺ efflux from the neuron through Gα_{i/o}, shunting excitation (28). The GIRK channels are built up by different subunits (GIRK1-4) that form either homotetramers or heterotetramers in a 2:2 ratio between two selected subunits. GIRK1-3 are expressed in the CNS, while GIRK4 is predominantly expressed in the heart. The GIRK1/2 heterotetramer is the most common within the CNS (28,29). The GIRK subunit components in a tetramer determine the channel efficiency and difference in localization determine the formation of specific tetramers, and thereby tune the efficiency of GIRK activity in specific tissues (29). GIRK channels can also be activated through direct binding to Gβγ and forming a complex utilizing cofactor phosphatidylinositol-4,5-biphosphate (PIP₂) (28). Similarly to the Gα pathway, this activation

scheme also causes slow hyperpolarization through GIRK K^+ -transport. However, this association is enhanced by the stabilizing effect of PIP_2 (28,29). In contrast to GIRK channels, the VGCC channels depolarize the membrane when activated. Upon activation through favoured membrane potential and voltage stimulation the VGCC channels assert an open confirmation and allow Ca^{2+} influx (28,30). Additionally, as noted in a previous section, Ca^{2+} is essential for vesicle membrane fusion of neurotransmitter-filled vesicles for neurotransmitter release into the synaptic cleft. $G\alpha_{i/o}$ signalling through $GABA_B$ -R stimulation effectively inhibits the VGCC (28). VGCCs are divided into the subfamilies L- (long lasting), P/Q- (Purkinje), N- (Neutral), R- (Residual), and T-type (Transient) channels, differentiated by location and voltage preference and built up by different combinations of subunits (28,30). In postsynaptic neurons, this mechanism effectively reduces the excitability of soma dendrites, and halts depolarization; while in presynaptic neurons, the predominant mechanism hinders Ca^{2+} influx to hinder fusion of vesicle membranes. $G\beta\gamma$, similarly with GIRK, has also been found to bind to VGCC channels, creating a inhibitory $GABA_B$ -R-VGCC complex (30).

The $GABA_{B1}$ subunit can also be found in two different forms: the $GABA_{B1a}$ and $GABA_{B1b}$. Which function identically on a protein level, but are found at different locations of the neuron, giving different roles. The B1a subunit is the only subunit which contains sushi domains, protein markers, that are recognized and translocate the protein towards the presynaptic end, the axon terminal (31). Thereby, only the B1a subunit is found at the presynaptic terminal, while both are found on the postsynaptic terminal; although only B1b is located on the spines, which are dendritic regions stretching from the axon itself. For clarity, from this point on $GABA_B$ -R refers to a heterodimerisation of the B1b -subunit and B2 -subunit (31).

1.3.2 $GABA_B$ receptors outside of the CNS

The importance of $GABA_B$ -R goes beyond the CNS. Multiple tissues and organs have been found to contain messenger ribonucleic acid (mRNA) of GABA receptor subunits utilizing reverse transcriptase. Including, but not limited to, the heart, gonads, gastrointestinal system, and the urinary bladder (32–39), whether they are neuronal cells or not (38,39). However, only the $GABA_{B1}$ subunit was found at higher levels, while the B-2 subunit was either undetectable or at low levels. Suggesting that the presence of heterodimeric receptors is at lower levels in these organs and systems.

1.3.3 GABA_B receptor compounds

The GABA_B-R has been connected to a range of psychiatric disorders, including but not limited to depression, anxiety, addiction and schizophrenia (25,40–42). Defects in GABA signalling and within the GABAergic system have a causal contribution to development of major depressive disorder, this idea is known as the GABAergic hypothesis (40,43). In addition, common antidepressants treatment ability is directly dependent of their ability to restore GABAergic neurotransmission and signalling balance (43). Other clinical applications investigated use of GABA_B-R drugs for epilepsy, sleep disorders, spasticity, analgesia, immunomodulation, digestive disorders, and as mucus inhibition and/or bronchorelaxation in asthma (44).

Over the last decades a variety of drug discovery attempts have been made to find GABA analogues with similar pharmacological effect and preferred physiochemical properties for therapeutic application of a GABA-like antidepressant drug. Utilizing the structure of GABA and the binding pocket of GABA receptors, multiple GABA analogues have been discovered, some of which are shown on **figure 7**. In addition, a variety of compounds were made in which endogenous GABA is an intrinsic part of the molecular structure, such as baclofen (45). However, despite the uncanny similarity to endogenous GABA, the target for these compounds are varied and some have no effect on GABA pathways (45).

As of 2021, there is currently only one drug targeting the GABA_B-R, the agonist baclofen (25,45). Baclofen is composed of the GABA backbone with an added phenyl ring structure, making it a hydrophobic variant of GABA. Aided by the large amino acid transporter, baclofen accumulates in the brain. However, baclofen's short half-life, short effect duration, narrow therapeutic window, and high instance of receptor tolerance excluded it from use within the brain (45). Though baclofen is in use today as an intrathecal muscle relaxant. From there, several GABA and baclofen analogues have been made, such as phenibut, pregabalin, vigabatrin, gabapentin, and lesogaberan. However, neither of these posed as better candidates for regulating GABA_B-R; although pregabalin, vigabatrin, and gabapentin have all been clinically approved for use as anticonvulsants, and pregabalin is also in use as a neuropathic analgesic, all of which without interacting with GABA_B-R directly (25,45).

In the last decades, the search for allosteric modulators has increased exponentially. The first allosteric modulator CGP7930 was discovered in 2001, and thorough testing also found that CGP7930 has agonist-like effect without access to endogenous GABA (25,46). Several other

modifiers have been investigated by the same means, from which GS39783, ADX71441, and CLH304a emerged (25,47). But similarly, these compounds have yet to show promise for clinical use.

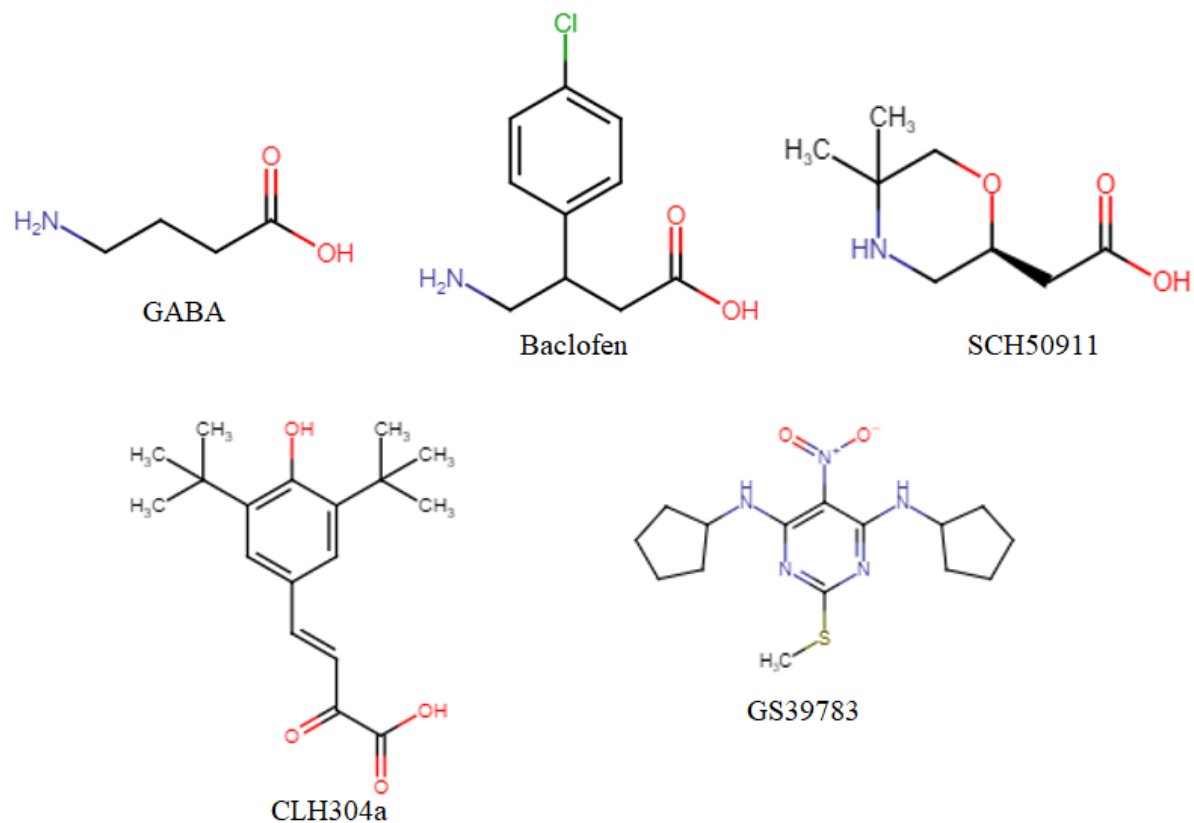


Figure 7: Exemplary structures that interact with GABA_B-R. From top left to bottom right; endogenous GABA binding orthosteric site, agonist baclofen, antagonist SCH50911, negative allosteric modulator CLH304a, and agonist-like positive allosteric modulator GS39783. Evidently the orthosteric binders shown all contain a GABA-backbone.

1.4 Blood-brain barrier and drug distribution to CNS

The blood-brain barrier (BBB) is the innermost physical barrier walling out external foreign material from the cerebrospinal fluid and the cerebral neurons it encapsulates. The BBB is made up of endothelial cells enforced by tight junctions, so that any molecule moving past the barrier must move through the endothelial cells. Although the barrier serves as a physical wall, it also contains transport proteins dedicated to blood-to-brain transport and brain-to-blood transport (48). Importantly, these transport routes also bounce back molecules from the blood that may not enter the brain, an efflux system.

The BBB rejects a vast majority of molecules, both restricting the entry and efflux of molecules that have entered the brain. Because of this, it is difficult to find pharmaceuticals with neurological activity that can pass the BBB successfully (49). To emphasize this, the active efflux of molecules from the cerebrospinal fluid over the BBB and into the blood is more efficient than the passive transport from the cerebrospinal fluid and into the brain (49). Meaning that drugs injected into the cerebrospinal fluid, will in a larger degree travel out into the bloodstream instead of into the brain.

1.5 Allosteric modulation

The search for allosteric modulators as therapeutics within CNS pharmacology, and GABA_B-R specifically, is a relatively new idea. However, the idea of allosteric modulation has been known for almost 60 years and was described in the works of Monod et al. (50). Already by then they suggested the idea of allosteric modulator induced changes in protein conformation by tertiary structures of the protein, complex changes in α -helix and β -sheet orientation within a polypeptide and related to the multi-polypeptide protein structure.

Allosteric modulators are compounds which bind to allosteric sites and modulate the enzyme or receptors without intrinsic activation or inhibition, in contrast to regular agonist or antagonist respectively, or inverting the effect such as an inverse agonist (26,51,52). Allosteric modulators bind to allosteric sites, which are any and all sites that are not associated with the endogenous ligand, the orthosteric site (26,51–54). Accompanying this, the allosteric site is commonly not a highly conserved region of the receptors, which is an important feature of the site as it allows for more selective allosteric modulators than was previously achievable with orthosteric ligands in pharmacological approaches (53,54).

The main therapeutic advantages of allosteric modulation of receptors come from their mechanism of action. Orthosteric ligands intrinsically activate the receptor whenever it binds and interacts with the receptor similarly to the endogenous ligand, while allosteric modulators provide a less direct effect by enhancing or halting the efficacy and/or affinity of the endogenous ligand to the receptor (26,53,55). By acting in line with the receptors' natural activation scheme, the pharmaceutical is expected to be tolerated at a higher degree and the prevalence of adverse effects to be reduced significantly (26,55). Orthosteric ligands, like the endogenous ligand, bind the orthosteric site and thereby compete for binding (51,55). Which is more problematic when agonists and antagonists compete rather than ligands with similar intrinsic activity.

Allosteric modulators are divided into three main groups: the positive (PAM), negative (NAM) and silent allosteric modulators (SAM). PAM and NAM structures will respectively enhance and halt the effects of the endogenous ligand (26,51). Thereby, the PAM strengthens the effects of an endogenous agonist, while the NAM weakens the effect. In the case of GABA_B-R, the endogenous agonist GABA stimulates the receptor and the receptor transmits an inhibitory effect, meaning that the PAM effect would be enhancing the inhibiting effect of the GABA_B-R when the receptor is bound to GABA. The first GABA_B-R PAM structures were discovered and described in the beginning of the present century (46,56). Following these, multiple new allosteric modulators have emerged, and recently the first NAM structure has been described (26,57). However, there are currently no allosteric modulators of GABA_B-R in clinical use. SAM structures are different from PAMs and NAMs. Despite binding the allosteric site, SAMs neither enhance nor halt the effect of the endogenous ligand. Instead, SAMs remain silent, or neutral (58). The main feature of SAMs thereby seems to be their ability to bind to allosteric sites, and therefore compete, with other allosteric modulators (26,58). A recent study of the mGlu5 receptor discovered a SAM with a significant pharmacological effect, without contributing to efficacy or efficiency of glutamate signalling. The SAM impaired mGlu interaction with pathological prions in Alzheimer's mouse (59). This suggests a putative use of SAMs in future pharmacological prospects.

1.5.1 Agonist- and antagonist-like allosteric binders

Allosteric modulation is not a strictly binary system. A modulators affinity to an allosteric site does not exclude its potential for intrinsic effect. Some allosteric modulators share features with orthosteric agonists and antagonists (58). These modulators create sub-groups of PAMs and NAMs. The notable groups that have been described are the agonist-like PAM (ago-PAM), and strangely the agonist-like NAM (ago-NAM), and antagonist-like PAM (PAM-antagonists) (58). **Figure 8** depicts the relationship between PAMs, NAMs, ago-PAMs, ago-NAMs, PAM-antagonists, and SAMs, and the orthosteric ligand (60). The ago-PAMs differ from standard PAMs by having intrinsic effect upon the receptor, while also differing from agonists by having positive allosteric effects with access to endogenous ligands. While ago-NAM and PAM-antagonist seem counterintuitive, their effects reflect their classification by respectively decreasing and increasing efficacy, while also increasing and decreasing the maximum output of the receptor (60).

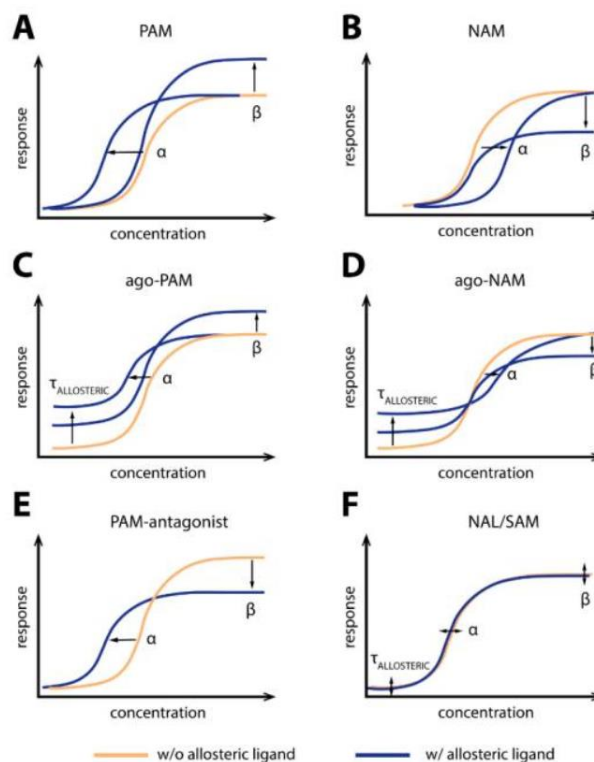


Figure 8: Illustrates the relationship between classifications of PAMs, NAMs and SAMs, and the endogenous ligand on a dose-response curve, with marked EC_{50} (α) and EC_{100} (β) values. A. Classical PAMs increase the efficacy of ligands and/or efficiency of the receptor when ligands are bound. B. Classical NAMs decrease the efficacy of ligands and/or efficiency of the receptor when ligands are bound. C. ago-PAMs increase the efficacy of ligands and/or efficiency of the receptor regardless. D. ago-NAM decrease the efficacy of ligands when bound and increase the efficiency of the receptor when low concentrations of ligands are present. E. PAM-antagonists increase the efficacy of ligands when bound and decrease the efficiency of the receptor regardless. F. SAMs commonly does not alter efficacy of ligands or efficiency of receptors. Figure adopted from (60).

1.6 In Vitro methods

In vitro assay is one of the three main research methods of pharmacological research, the two others being *in vivo* and *in silico*. *In vitro* specifically comes from Latin, meaning “in glass”, describing the fundamental part of *in vitro* experiments. Commonly, these methods utilize cell tissues or isolated cell lines, and are conducted in controlled environments such as test tubes or microplates (61).

In the present study. Experiments were conducted using a genetically modified (GMO) variant of the Chinese hamster ovary (CHO) cell line, namely the CHO-K1 cell line expressing GABA_B-R.

1.6.1 Cell culturing

There are three main classifications for *in vitro* method. Tissues, organ fragments, and whole organs; primary cultures; and cell lines (61,62). Tissues and larger structures are directly taken from animal or human donors and put to use immediately. Which also in part make them difficult to standardize, since there are differences between individual donors (62,63). Additionally, these structures require a more complex environment. Tissues will be extracted for use in applications when structural and functional features of the donated tissue is required, such as the use of thin slices of organ tissues (63). A primary culture refers to the cells and/or tissues deriving directly from donors. These cells more closely resemble those *in vivo*, within the individual, and are therefore highly applicable. Primary cultures are heterogenous systems with limited lifespan and additionally differentiate over time. This creates an uncontrollable variation between cells, cell cultures and thereby application results (62,63). The last method utilizes cell lines, which are subcultured primary cultures and are further subdivided into the subclasses finite cells, continuous cells and stem cells (63). Much alike primary cultures, finite cells have a limited lifespan, and will cease proliferation after 60-70 population doublings. Despite still being viable post-senescence, these cells alter their own nature and introduce variance with these changes. Continuous cells differ from finite cells by that they can be subdivided indefinitely and cannot reach senescence. However, these cells can also go through irreversible changes. Therefore keeping passage conditions constant is pivotal to maintain continuous cells (63). Stem cell lines, and specifically embryonic stem cells, inhabit the ability to differentiate to any other host cells. Retaining this capacity requires accurate maintenance and tailored cellular environment (63,64).

1.6.2 Chinese Hamster Ovarian (CHO) cells

The CHO cell line is one of the first ever stable immortal mammalian cell lines, designed by award winning Dr. Theodore Puck in the 1950s (65). Ever since then the CHO cell line has been a staple research target and is widely used around the world. Multiple efforts have been made to improve the cell line. Most notably the removal of dihydrofolate reductase (DHFR), making the cell line reliant on added glycine, hypoxanthine and thymidine to survive (DG44 CHO), which can be utilized as an advantage when creating recombinant cell lines such as the CHO-K1 cell line expressing GABA_B-R (66). Over the recent decades optimization of the cell line and improve selection strategies have been widely adopted (65).

1.6.3 cAMP accumulation assay

A cAMP accumulation assays utilizes the intracellular concentration of cAMP as an indication for pharmacological activity upon stimulation. This is applicable in multiple different procedures, such as monitoring cAMP dependent enzyme PKA, cAMP activated transcription factors, and more preferably measuring cAMP concentration directly using a luminescent approach (67). The latter procedure has been favoured in pharmacological research due to the safety, cost efficiency and highly repeatable results.

cAMP, or 3',5'-cyclic adenosine monophosphate, is the cyclic variant of AMP and is converted from ATP by the highly regulated AC enzyme. Regulation of AC is predominantly by GPCRs utilizing G α_i and G α_s which respectively inhibit and stimulate cAMP conversion by the AC (68). Consequentially, this means that the intracellular level of cAMP is directly related to AC-activity and thereby related to GPCR activity, of which is used as a tool for this study.

Utilizing the cAMP pathway endpoint, measuring the gene expressional change by cAMP response element (CRE) gene. Phosphorylation of CRE-binding (CREB) proteins initiates the binding and expression of CRE genes. Expressed CRE as a promoter will then regulate fluorescent or luminescent proteins, or an enzyme, to produce the selected readout related to the amount of cAMP (55). The major drawback of this method is that the product or readout is measured far downstream from the initial effect, being the receptor binding. Which means that multiple cellular regulation systems are included and can affect the final readout, potentially diluting or masking the effect of the receptor. Especially, since both AC and cAMP affecting more than one pathway (69). One can also utilize anti-cAMP antibodies that bind cAMP competitively against the alternative radioisotope 125 iodine ([¹²⁵I]) labelled cAMP. The

amount of bound cAMP will then be directly related to total cAMP in the cell, when the free unbound [¹²⁵I]-cAMP is filtered out.

The present study utilizes another method displayed on **figure 9**, the HitHunter® cAMP Assay for Biologics and Small Molecules from DiscoverX Products. With this method, the endogenous cAMP competes for anti-cAMP antibody binding with added cAMP bound β -galactosidase (β -gal) fragment, known as an enzyme donor (ED). The remainder of the β -gal, the enzyme acceptor (EA), will only bind free cAMP-ED to complete a full β -gal enzyme. The complete enzyme then catalyses the formation of a chemiluminescent product from added substrate. Additionally, as the experiment uses live cells, a reagent to break apart the cells and reveal intracellular cAMP for anti-cAMP antibody binding is used. See Methods section for protocol.

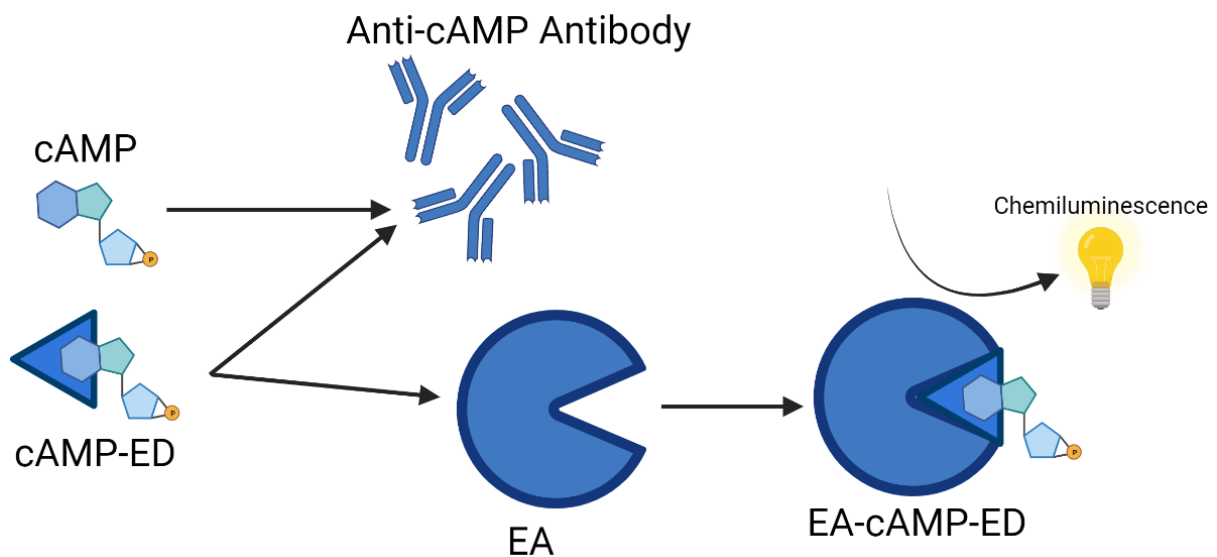


Figure 9: DiscoverX's cAMP accumulation assay. The assay kit includes cAMP Antibody Reagent, containing anti-cAMP antibodies; cAMP working solution, containing lysis buffer, cAMP-labelled β -galactosidase fragment enzyme donors (cAMP-ED), and enzyme substrates; and cAMP Solution A, containing β -galactosidase enzyme acceptors (EA). Endogenous cAMP and cAMP-ED compete for binding of anti-cAMP antibody. Outcompeted cAMP-ED bind to EA and manufactures functional enzyme. Functional enzyme utilizes substrates to create measurable chemiluminescence. Chemiluminescence is thereby relative to functional enzyme amount, which is relative to free cAMP-ED, which again is related to out-competition by cAMP; Thereby chemiluminescence is directly related to concentration of endogenous cAMP. Created with [Biorender.com](https://www.biorender.com).

1.6.4 Radioligand-binding assay

Radioligand-binding assay, or receptor binding assay, is an *in vitro* method utilizing cell membranes and a filtration system which aims to obtain information on ligand affinity to a receptor and ligand interactions with the receptor in absence and presence of other ligands (70). There are several fundamental approaches to a binding assay that yield distinct information on ligand binding to the receptor. The first approach is by adding ligand onto the cell membrane preparation and taking measurements over time at several increments to achieve information on association and dissociation kinetics between receptor and ligand. Additional information on kinetics can be achieved by utilizing several concentrations of the ligand. The second approach also utilizes the general idea, but at saturation to analyse rate constants. Finally, the third approach aim to investigate the radioligands ability to compete or cooperate with a secondary non-labelled ligand at increasing concentrations. Both ligands are given equal opportunity to bind the receptor alongside a control with only radioligand, and binding of radioligand is measured (70).

In this study, radioactive [^3H]GABA that binds to the orthosteric binding site is utilized as a control to verify whether test compounds bind to allosteric sites or the orthosteric site in a filtration-type radioligand binding assay. A ligands ability to displace [^3H]GABA from the receptor can then be studied.

2 Aim

Baclofen is currently the only approved clinical drug targeting GABA_B-R, however due to several limitations and its adverse effects it's not applicable for use within the human brain. Several GABA and baclofen analogues, with agonist or antagonist functions, have been studied. But none of these have shown promise for application within the brain either. This has led to the investigation of allosteric modulators in PAMs and NAMs. PAMs/NAMs do not possess intrinsic ability to stimulate or inhibit the receptor and will instead modulate the receptors activity when bound to GABA, tuning the stimulation by either increasing (PAM) or decreasing (NAM) the receptor activity. GABA_B-R modulators display several advantages over orthosteric ligands, such as: binding highly specific allosteric sites, do not compete for a orthosteric binding site, and has a weaker effect on receptor signalling.

We have previously identified GABA_B-R modulators through both virtual screening and the cAMP accumulation assay tests. However, the previous cAMP assay protocol had poor assay repeatability. Therefore, the main aim of the present thesis is to improve the method so that satisfactory repeatable results could be achieved. Furthermore, we wanted to use the optimized assay protocol to test several newly synthesized structural analogues, as well as re-evaluate previous hit compounds.

Additional aims were to master all basic experimental techniques needed for this study, such as: cell culturing, cAMP accumulation assay, radioligand binding assay, and use of various lab instruments.

3 Material and Methods

The experimental method followed and adjusted the manufacturer's instructions. The following materials were purchased from DiscoverX: CHO-K1 wild-type cell line was provided by Tumour biology research group at UiT The Arctic University of Norway. cAMP Hunter™ CHO-K1 GABAB1+GABAB2 Gi Cell Line (cat.# 95-0165C2). AssayComplete™ CHO-K1 Cell Culture Kit 35 (cat.# 92-0018G2R2) which has medium, serum and antibiotics mix (Pen/Strep/Glu, Geneticin and Puromycin). AssayComplete™ Freezing Reagent F2 (cat.# 92-5102FR). AssayComplete™ Revive CHO-K1 Media (cat.# 92-0016RM2S). AssayComplete™ Cell Detachment Reagent (cat.# 92-0009). HitHunter® cAMP Assay for Small Molecules (cat.# 90-0075SM2). White bottom, tissue culture treated 384-well (cat.# 92-0015). Chemicals purchased from Sigma-Aldrich are: NaCl (cat.# 746398), KCl (cat.# 746436), D-(+)-Glucose (cat.# G7021), CaCl₂ (cat.# C7902), MgCl₂·6H₂O (cat.# M9272), HEPES (cat.# H3375), NaOH (cat.# 30620), GABA (cat.# A5835), water soluble forskolin NKH477 (cat.# N3290), and DMSO (cat.# 472301).

The compounds for testing in the present study are shown in **figure 10** and appendix B, and were synthesized by our collaborators at the Maj Institute of Pharmacology, Polish Academy of Sciences. Most of the compounds are analogues of interesting hits from previous studies in the research group, but also some of the previous hits are included. The previous hits were identified using a combination of ligand-based and structure-based virtual screening utilizing a homology model of the receptor (71), and through the cAMP accumulation assay prior to the present thesis.

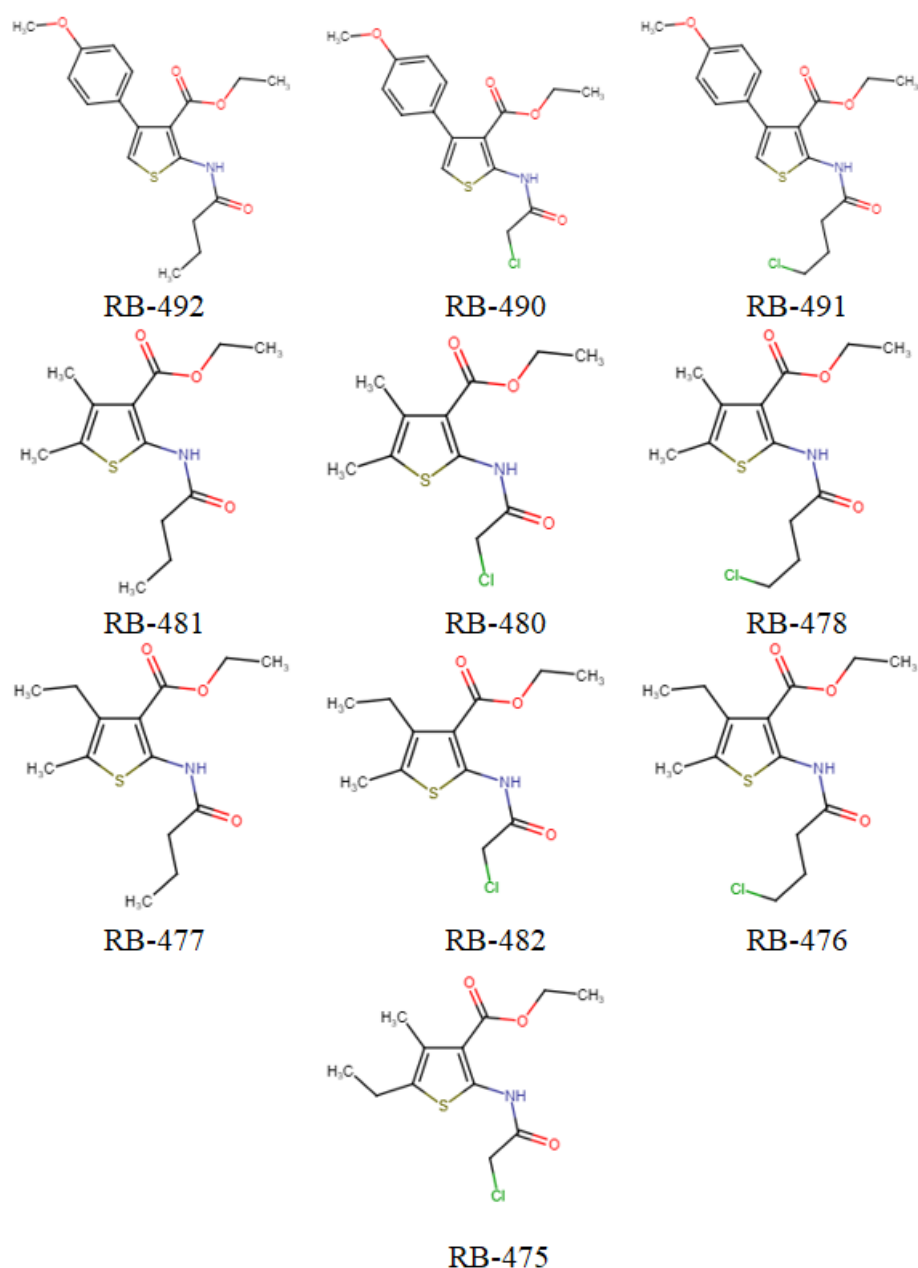


Figure 10: The RB-test compounds under investigation for allosteric modulation. Here presented in rows and columns where each compound shares chemical features in their grouped column and grouped row.

The solubility of these compounds was tested for a fully optimized cAMP accumulation assay. The compounds were dissolved in 10mM stock concentrations by using 100% DMSO. The stock solutions were then preserved in -20°C . The compound solubility test shows that all compounds have better solubility in a solution containing NaOH and D-Glucose. RB-490, RB-478, and RB-481 were soluble as $24\mu\text{M}$; RB-492, RB-491, and RB-477 were soluble at $12\mu\text{M}$; and the remaining RB-480, RB-482, RB-475, and RB-476 were soluble at $6\mu\text{M}$. Their final in-assay concentrations would then be $4\mu\text{M}$, $2\mu\text{M}$, and $1\mu\text{M}$ respectively.

3.1 Cell culturing

This study utilized two cell lines: CHO-K1 cell lines that carries GABA_B-R and wild type CHO-K1 cells. These were cultured following guidelines from DiscoverX, though some adjustments were made for optimal assay condition. Cell culture procedure was described in **figure 11**. Both Phosphate-buffered saline (PBS) and cell culture media (See Appendix A for recipe) were prewarmed for 15 minutes at 37°C. The wild type cells were cultured with different culture media and incubation periods of ~37 hours due to their fast growth rate.

On the first day of culturing GABA_B-R cells, frozen cells stored in liquid nitrogen were thawed in 37°C water bath for about 1 minute. When a small pellet of ice remained, the vial was immediately removed from water bath to avoid overheating of the cells. Fully thawed cells at room temperature were then collected and immediately put into 10mL of prewarmed culture media, which followed by a centrifuge spin-down at 300G for 5 minutes (the standard used for all following centrifugation). Supernatant was aspirated using point suction and the cell pellet was gently resuspended in 15mL culture media. Thereafter, the cells were seeded in 5ml per T25 flask format. To make sure an even distribution of cells, the cell culture flasks were rocked 8 times on both x and y axis of the flasks. The cells were left to sink for 5 minutes on the bench before they were put into 37°C cell culture incubator. Cell seeding density were adjusted to a 48 hours cell splitting cycle.

Right before next cell splitting, the cells were evaluated under a microscope to ensure that the cell confluency was around 80-95%. Once optimal cell confluency was reached, the cells were then washed three times using prewarmed PBS and subsequently detached using DiscoverX's detachment reagent. Detached cells were washed down with PBS and collected into a 50ml centrifuge tube. The tube was centrifuged at 300g for 5 minutes, supernatant aspirated and cells resuspended into 4mL of culture media. The cells were counted in an automatic cell counter using trypan blue method. Once the cell concentration was determined, around 1.2-1.5 million cells were seeded into one T75 flask. The cells were evenly distributed in the T75 flask before they were put into incubator for another 48 hours cell growth.

Once the cells reached confluency of 80-95%, the cells were washed three times with prewarmed PBS and detached using detachment reagent. Harvested cells were resuspended in culture media to 1 million/mL concentration. Around 3.3-3.5 million cells were seeded into a T175 and ~1.2-1.5 million cells into a new T75. Cells were evenly distributed in the culture flasks and put into the incubator for another ~48 hours cell growth at 37°C.

At this stage, cells in both T175 and T75 flasks would reach desired confluency after 48 hours. At the day of assay, cells in T75 flask were split into one T175 flask and one T75 flask as described above. However, the harvested Cells from T175 were prepared for cAMP assay. Briefly, cells in T175 flasks were wash 3 times with prewarmed PBS, harvested in 40ml PBS. After centrifugation, the cell pellet was washed once in 1x Hank's balanced salt solution (HBSS) buffer (see Appendix A for recipe) and resuspended again in 20ml 1x HBSS buffer. This gave us a cell concentration of approximately 0.9 -1 million cells/ml.

Cell culturing

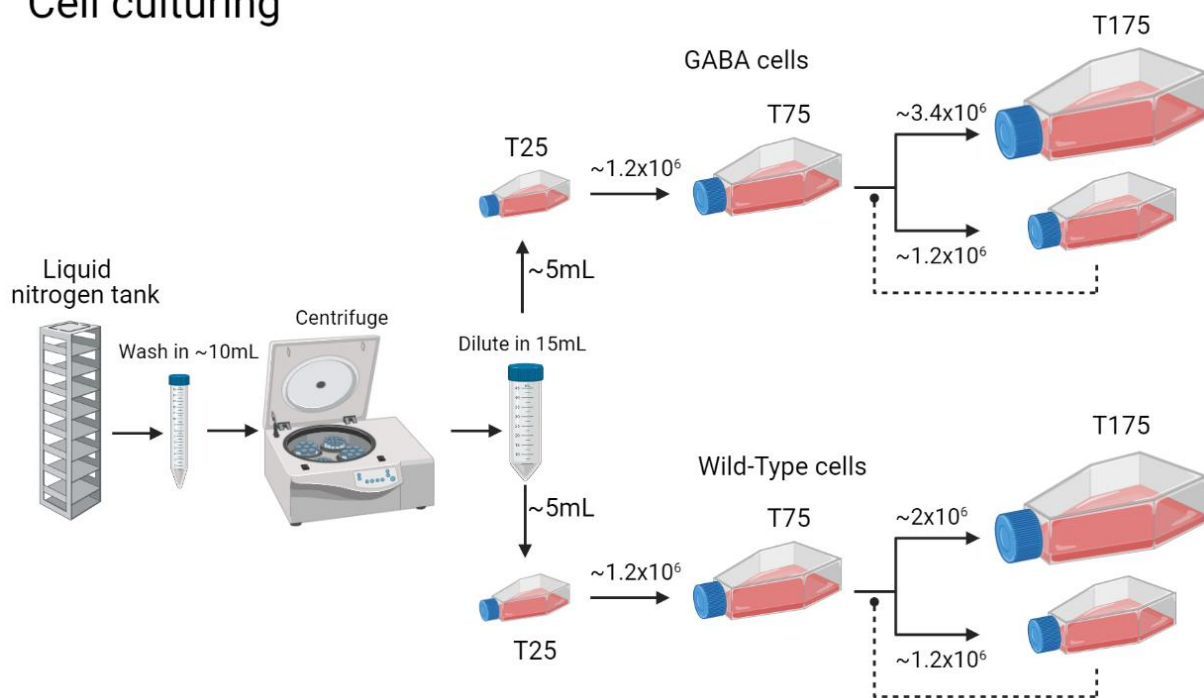


Figure 11: Cell culturing splitting regime with relative cell counts for each flask with both Wild-Type and GABA cells. Cells are stored in 1mL vials submerged in a liquid nitrogen tank. Starting cell culturing, a vial is withdrawn, thawed and washed in serum. Cells are pelleted, supernatant aspirated and diluted with serum. A T25 flask is seeded with 5mL of this solution and left for incubation for 48 hours (36 hours for Wild-Type). When T25 flask reaches confluency of ~80-95% it is washed, cells detached and collected, and spun down; supernatant aspirated, diluted in media respective to confluency, and set amount is seeded into T75; T75 is topped off with media to 15mL total volume and put into incubation for 48h. T75 is treated similarly to T25 with increased volumes, and cells are seeded into a T175 and new T75 to repeat the cycle. Both are incubated for 48 hours, to which T175 is ready for harvest and assay. Created with [Biorender.com](https://www.biorender.com).

3.2 cAMP accumulation assay

Our cAMP assay was conducted using suspension cells. At the day of assay, the harvested cells were first incubated for 2.5 hours at 25°C in a water bath. During this incubation time, 40mM stock GABA solution in 2x HBSS buffer were prepared. Followed with creating a serial dilution of GABA as illustrated in **figure 12**. GABA dilution Nr 4 and Nr 7 were used as GABA_{EC20} and GABA_{EC80}, respectively. The 5mM Forskolin stored in pure water were diluted to 360µM in 2xHBSS buffer. The test compounds were prepared in 5G solution (See appendix

A for recipe) describe above at their highest soluble concentration. Lastly, GABA, forskolin and test compounds were mixed as shown on **figure 13**.

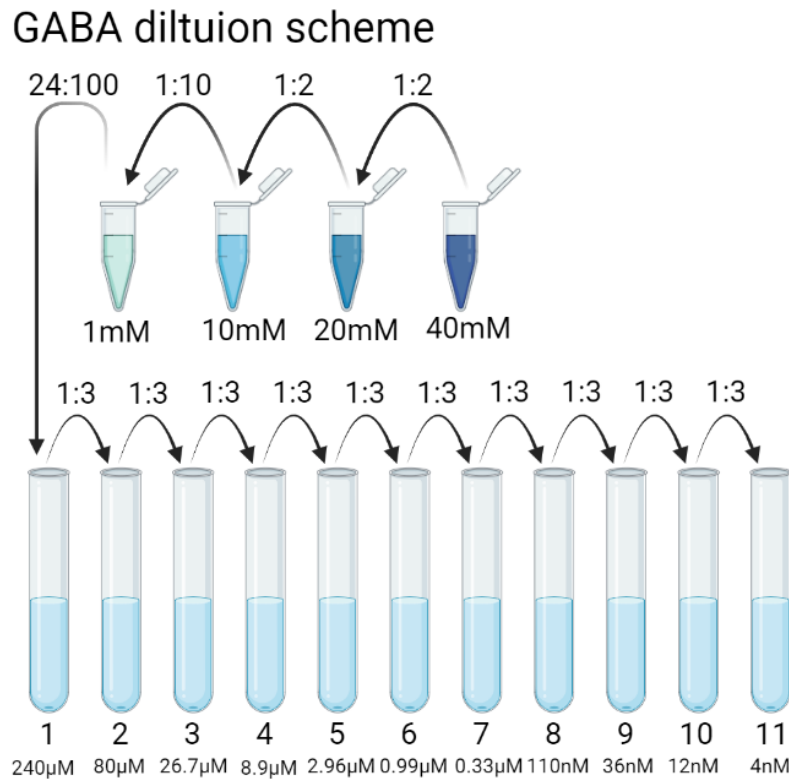


Figure 12: GABA dilution scheme. GABA is weighed out and dissolved in 2xHBSS to 40mM. From there it's diluted 1:2 to 20mM and further to 10mM. Followed by further dilution by 1:10 and 24:100. For 24:100, in which 960µL in 4mL total volume was used. This dilution of 240µM is named Nr.1 and serves as the highest concentration of GABA in a dose-response curve. Thereafter a 1:3 serial dilution was conducted 10 times to concentration Nr.11. Created with [Biorender.com](https://www.biorender.com).

To avoid any crystallization issues, the test compounds dilution was prepared just a few minutes before assay start. Final concentration of forskolin in the assay is 30µM. This corresponds to around 80% of maximum stimulation (data not shown). The forskolin stimulated cAMP accumulation mechanism is shown on **figure 14**.

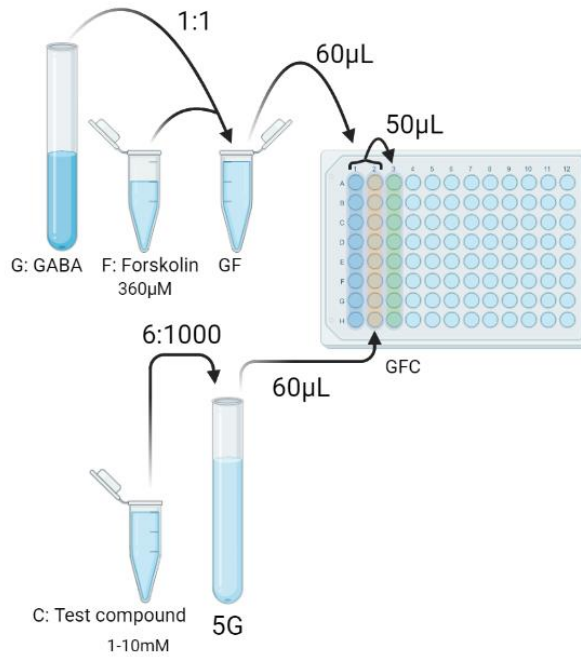


Figure 13: The GABA-Forskolin-Compound (GFC) mixture is made by first combining GABA and Forskolin into a GF stock, as this concentration must be the same for each well to achieve comparability. Approximately 60µL of GF stock is plated out using a pipet onto each well on a 96-well microplate column. Once compounds have been diluted in 5G, these were in the same manner plated onto a second column. Then an eight-channel pipet was used to transfer 50µL of GF and thereafter 50µL compounds and mixed until homogenous. Created with [Biorender.com](https://www.biorender.com).

After 2.5 hours of cell incubation in 25°C water bath, cells were resuspended by gently shaking the tube and rested for 5 minutes before they were dispensed into the microplate preloaded with compound mixture. For cell dispensing, MultiFlo™ FX Microplate Dispenser was used. Once cells were mixed with compound mixture, microplate were incubated at 25°C for 25 minutes. After 25 minutes, cAMP reagent was added according to manufacturer's instruction. The microplate was left under dark for 12-14 hours before scanning of the chemiluminescent signal.

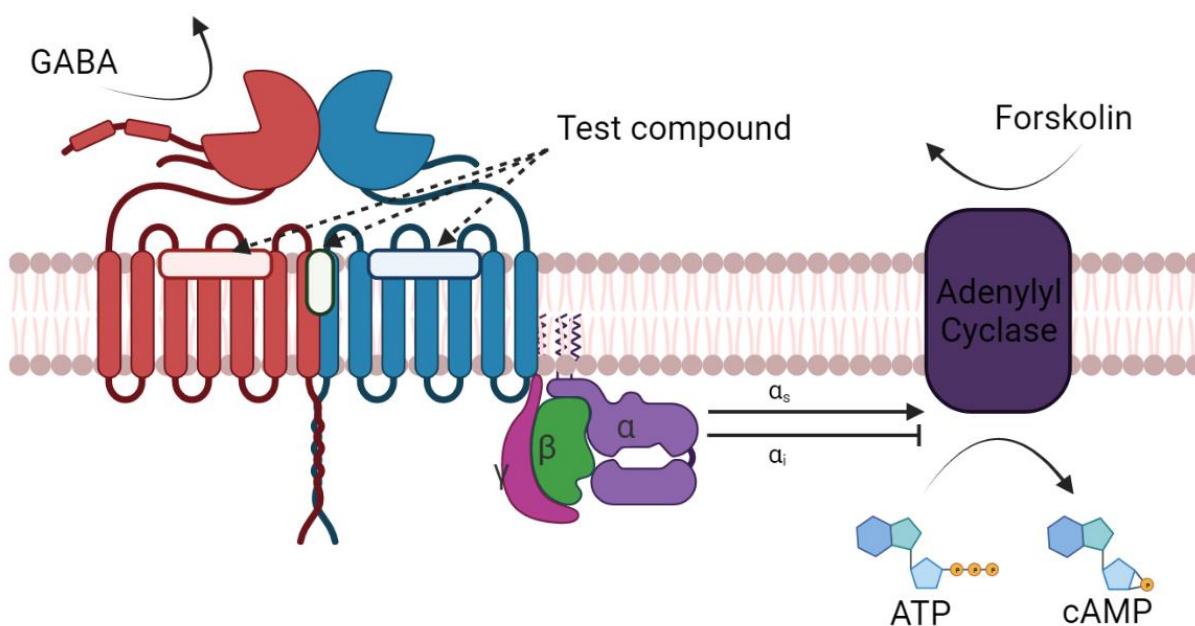


Figure 14: Test system used for functional cAMP accumulation. Adenylyl Cyclase (AC: purple) and G-proteins ($\alpha\beta$) are Wild-Type peptide complexes, while the human GABA_B-R (B1b in red and B2 in blue) are results of genetic modification. Forskolin, GABA and test compounds are added to the system initializing reaction time. Forskolin stimulates AC to almost maximize potential cAMP production, GABA activates GABA_B-R which mediates inhibition of AC through G α_i . Test compounds can mediate changes in endogenous cAMP through a variety of cellular mechanisms, however accompanying GABA with Wild-Type assay the system excludes non-GABA_B-R functions; and subsequent radioligand binding assay excludes orthosteric binding, leaving only the three allosteric sites as possible binding positions. Created with [Biorender.com](https://biorender.com).

3.2.1 Prerequisite factor-dependent assay

To establish a repeatable functional assay, several assay conditions must be determined first. These include assay temperature, reaction time, forskolin concentration, compound solubility, DMSO tolerance, incubation time, cell quality, cell concentration, etc. A pre-determined assay condition usually can be found either from literature or manufacturer's instruction of the assay reagent used. However, due to the difference from lab to lab, one must determine some critical assay conditions locally. Such as, a forskolin dose-response assay can show us what is the best forskolin concentration we can use in compound testing, so that it gives the best assay window for both NAM and PAM screening. On the other side, a time-dependent assay of forskolin-stimulated cAMP accumulation can show us what is the best reaction time. Since our cAMP assay is based on live cells, it is also necessary to do a temperature-dependent forskolin stimulation assay. Ideally, physiological temperature (37°C) should be the most natural option. However, performing an assay with limited instrument made assay at physiological temperature is hard to achieve. Besides, a microplate edge effect and the reagent dispensing speed will also affect such an assay. Therefore, cAMP assay at room temperature could give us more flexibility.

3.3 Assay optimization

By thoroughly testing the cAMP accumulation assay through both compound testing and creating GABA dose-response curves (results not shown) it was quickly discovered that the method did not yield satisfactory repeatability. Over the course of almost a year the method was therefore under inspection and optimization.

The first identified issue is microplate edge effect. The outer rim of the 384 well microplate yielded much higher signal than the wells at the centre. This was confirmed by switching positions for test compounds on the microplate, namely the compound placed on the edge of the microplate would show a NAM-like, inverse agonist-like or antagonist-like effect, depending on whether control samples were also placed on the edge of the microplate or not. The issue might be related to the internal heating system of the microplate reader. Although switching off the heating system slightly improved assay results, it did not eliminate the discrepancy completely. A new strategy to avoid any use of the edges of the microplate was also tested. However, the microplate edge effect remained to some extent due to intrinsic temperature differences between wells across the entire microplate. This intrinsic temperature difference was discovered using an infrared thermometer.

The temperature dependency of the cAMP accumulation assay performed by others within the research group (data not shown) have verified the sensitivity of cAMP accumulation to temperature variation. Therefore, keeping a stable temperature during the reaction time became our primary goal. One solution could be submerging assay microplate in water bath during the 25 minutes reaction time. However, new issues showed up in these tests. Firstly, most white opaque microplate used for chemiluminescent assay are flat bottom. When such microplates were put in water bath, the microplate plastic gradually warm up from bottom to top. Since our assay used cell suspension, this could create different reaction speed between wells on the edge and wells located in the middle of the microplate. The actual assay results might be improved in terms of repeatability, however the microplate edge effect was still present. Secondly, when the microplate was put in a water bath, water around the microplate could accidentally splash into the microplate which made it very difficult to add cAMP reagent after 25 minutes reaction time. After numerous tests with stabilizing the microplate and controlling water speed inside the water bath, the issue was not solved. Since it is not possible to find an ideal microplate on the market that fits our need for temperature control. A new approach was adopted, which is to build assay microplate by ourselves. After careful design and construct, a 6-column glass well microplate was built. This microplate used the same structural dimension of standard 96 well

microplates. Unlike 12-columns 8-rows microplates, our glass microplate used 6-columns 8-rows format. For the wells, dozens of flat bottom glass inserts were put into place. The 6 columns were determined by choosing every other column of the standard 12 columns. This organized pattern made it easy for water in the water bath to flow freely and easily on both sides of the 6 columns, and therefore guaranteed to minimize the temperature difference between wells. Notable, the volume and size of each glass insert were carefully adjusted to meet both final assay mixture volume and compatibility with the MultiFlo™ FX Microplate Dispenser. Since this configuration will reduce the assay throughput from 96-wells to 48-wells, we therefore decided to use technical quadruplicates. This strategy immediately improved the assay repeatability (results not shown). Further improvements were made by changing pipetting strategies using different combinations of manual and electronic pipets, changing reagent orders, microplate post-incubation shaking speed, and style of mixing.

Although other tests were also done to increase the assay throughput from 48-wells to full 96-wells, the same microplate edge effect immediately returned. The failed test, on the other hand, showed us how sensitive the cells are to the temperature during the 25 minutes reaction time.

3.4 Radioligand binding assay

Establishing the radioligand method and creating a functional protocol was not part of this thesis. In principal, the assay aims to utilize a cell membrane preparation containing GABA_B-R and investigate whether test compounds could displace radioactive GABA bound to the orthosteric site. This is achieved by incubating the GABA_B-R cell membrane fractions with [³H]GABA and the test compound for a certain time, which is then followed by filtering out free radioligand from bound radioligand on a filtration system. The radioactivity was then measured on a plate reader.

Several previously made in-house equipment was utilized to conduct the radioligand binding assay. To summarize, the equipment is composed of four detachable layers with a standard 96-well dimension and formation at the centre: the first layer serves as a filtration unit which is hooked up to a suction to create negative pressure, the second layer is a loading plate for applying the filter membrane on top of it, the third layer is an assay mixture loading layer firmly attached on top of the second layer, and lasty the fourth layer which is a wash buffer loading layer that is attached directly on top of third layer. During the filtration procedure, all four layers will be sequentially and firmly attached to each other using four threaded stainless-steel rods. 96 silicon rings were fixed on bottom of third and fourth layer, which helps to separate

each of the 96 wells when assay mixture was loaded. Therefore, very tightly assembled layers are crucial to perform successful membrane filtration and washing steps.

Another advantage of this in-house built filtration unit is to use cheap filtration membrane sheets. Namely, a double layer 30cm x 300cm nitrocellulose membrane was bought and cut into exact dimension that can cover the 96 wells of the filter membrane loading layer. Before starting actual tests, we also determined the amount of cell membrane suspension from stock membrane solution that would be just good enough to avoid blocking the nitrocellulose filter membrane. Once this was determined, samples containing the set amount of membrane along with test compounds and radioactive tritium-GABA in assay buffer (see appendix A) were put into a 27°C water bath to incubate for 1-hour incubation.

After incubation, sample triplicates are loaded onto the filtration assembly and quickly washed with ice cold wash buffer (see appendix A). After filtering through the wash buffer, the equipment was disassembled, and the nitrocellulose filter membrane was carefully transferred onto in-house build microplate where the filter was left to dry for 24 hours.

On the next day, 20 µl MicroScint™-O scintillation cocktail was added to dried nitrocellulose membrane. The tritium β-rays could collide with the chemical components in scintillation cocktail and transfer energy to create measurable photons. These photons could then be measured using a Top Count® plate reader. The measuring time for each well on the microplate was 10 minutes. Due to the time constrain, only a test run of the binding assay was performed to prove the concept. Although all the filtration process was successful, the end results were not ideal (data not shown). However, a further optimization of the in-house built filtration unit in the future might solve the identified issue.

4 Results

4.1 Method

Optimization steps found temperature, mixing, and time usage to be of the utmost importance when conducting the cAMP accumulation assay. Additionally, precision pipetting could also impact the results and create differences between individual tests within the same day of assay.

A fully optimized functional method utilizing in-house equipment was established. The water bath maintained a constant temperature using a magnetic stir, thermometer and external heating. For cell dispensing, MultiFlo™ FX Microplate Dispenser played important role in keeping assay repeatability. Without this cell dispenser, it would be very difficult to establish the assay.

Reagents added directly after one another for each column in quick succession using electronic pipets gave the most promising results, although it is technically challenging. However, adding cAMP working solution within 30 seconds after adding antibody also gave good repeatable results. Preloading cAMP working solution and cAMP Solution A in glass columns put into the same water bath helped to maintain the temperature of final assay mixture, which also contribute to improved assay repeatability.

4.2 cAMP accumulation assay

Functional cAMP accumulation assay was done using the optimized method with brand new in-house equipment. As displayed on **figure 15**, compared to GABA EC80 control.

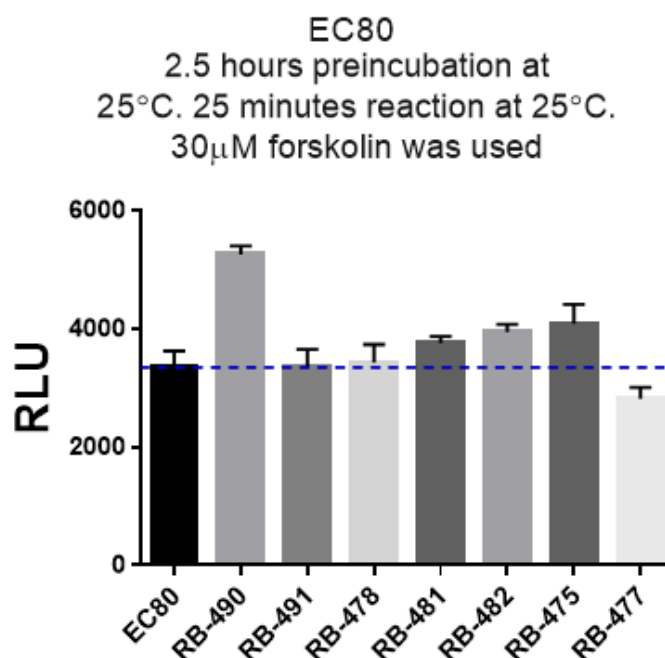


Figure 15: Compound test of named compounds in GABA_B-R cells with T-shaped standard deviation. GABA at EC80 concentration (Black bar and blue line) is used alongside 30µM forskolin. Cells were incubated for 2 hours and 30 minutes at 25°C, reaction time of 25 minutes, and assay was conducted at 25°C.

The compound RB-490 dramatically increased the relative light unit (RLU), or rather cAMP level. Compounds RB-481, RB-482, and RB-475 slightly increased the cAMP level, while RB-477 decreased cAMP level. Additionally, compound RB-476 posed similar results to RB-477 (results not shown). The remaining compounds, RB-491, RB-478, RB-480, and RB-492 did not alter the cAMP level significantly (some results not shown).

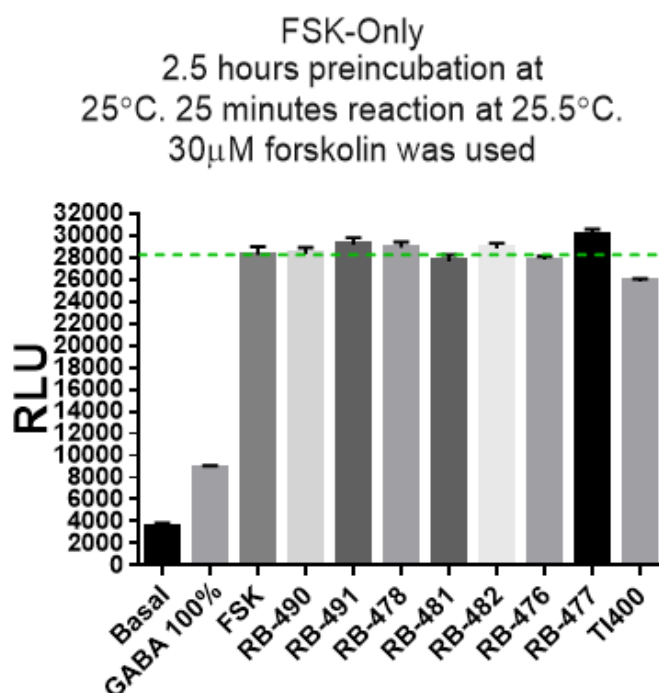


Figure 16: Compound test of named compounds in GABA_B-R cells with T-shaped standard deviation. GABA was not present and 30µM forskolin (FSK shown as grey bar and green line). Cells were incubated for 2 hours and 30 minutes at 25°C, reaction time of 25 minutes, and assay was conducted at 25°C.

In the absence of GABA, compounds were tested against forskolin (FSK, green line) stimulation only. The test, **figure 16**, showed that none of the compounds significantly and repeatedly affected the cAMP signal compared to the forskolin only control. Previously confirmed agonist-like TI400 was also tested. Although compound RB-477 may increase cAMP level, this result was only achieved once. Additionally, due to the optimization process, results in this particular assay have fluctuated between optimization steps and was not repeated on fully optimized assay procedure.

4.2.1 Wild-type assay

Wild-type assay was run on the CHO-K1 wild-type cell line (results not shown). The results indicate compounds RB-492, RB-481, and RB-477 increased the cAMP within 10% of the control. Additionally, compounds RB-480 and TI400 just slightly decrease the cAMP levels. The remaining compounds RB-490, RB-491, RB-478, RB-482, RB-475, and RB-476, did not show any effect on the forskolin stimulated cAMP levels.

4.2.2 Compound dose-response assay

A dose-response assay was conducted using compound TI400, shown on **figure 17**. The test included a standard GABA dose-response as a control, alongside three GABA dose-response curves containing TI400 in 10 μ M, 5 μ M and 1 μ M concentration. The curves show a decreasing cAMP level with each increase in compound concentration. In the presence of 10 μ M TI400, GABA_{EC50} dropped from 107nM to 40nM, indicating a PAM like effect of compound TI400.

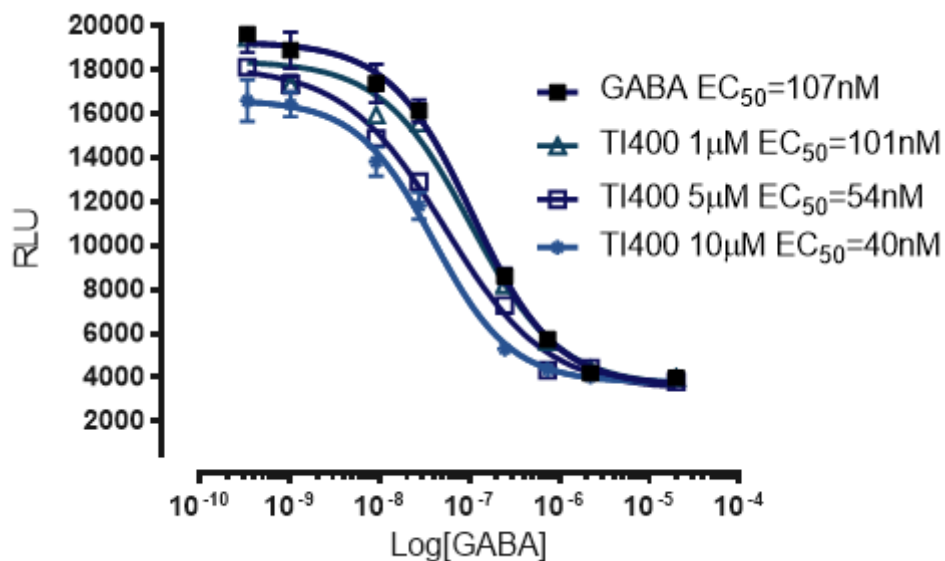


Figure 17: Representative compound dose-response of TI400 on a GABA dose-response. TI400 concentrations used in the experiment were 10 μ M, 5 μ M and 1 μ M. Increasing concentration of compound decreases the RLU and the apparent deviation from the GABA control.

5 Discussion

Allosteric modulation for clinical application within the CNS, specifically modulations of the GABA_B-R within the brain, innovated a new approach in drug design to target the GABAergic system. The allosteric site of GABA_B-R and other family C receptors have been found to be less conserved, meaning they are remarkably different to each other compared to orthosteric sites. This difference in shape and overall amino acid composition creates a more specific binding pocket which is a crucial advantage for drug targeting. A second critical advantage stems from the modulators function. Most allosteric modulators do not have intrinsic effect through the receptor and will only tune the receptors activity through orthosteric binding of endogenous ligands. Therefore, these allosteric modulators can finetune the cellular signalling that is triggered by endogenous orthosteric ligand binding. The aim of this study was to investigate possible allosteric modulators and determine their activity and binding pattern using a set of *in vitro* assays. In order to accomplish this, optimization of cAMP accumulation assay became our primary goal in this study.

5.1 Optimization

The use of suspension cell and water soluble forskolin made the cAMP assay both easier to perform with the available instruments in our lab and reduced the DMSO concentration in final assay mixture. Using forskolin concentration slightly lower than maximum system stimulation will ensure to detect negative allosteric modulator or possible antagonist.

Temperature differences was the most important issue in cAMP assay optimization. Difference in temperature affects not only the reaction speed of forskolin stimulated cAMP production, it also affects the maximal cAMP level for various controls. Without a good control, we can easily misguiding by false positive or false negative results of test compound. The use of a water bath with magnetic stir, constantly stirring from the bottom, not only helped to keep the temperature evenly distributed around glass microplate, it also helped distributing the heat from the bottom heater which holds the temperature to 25°C during the 25 minutes reaction time. The actual change of temperature in water bath was kept at $\pm 0.2^\circ\text{C}$.

After 25 minutes reaction time, two steps need to be done immediately: adding antibody reagent and adding cAMP working solution. Since both steps can be done by using electronic pipets, a time dependent assay of adding antibody solution was performed (data not shown). The results show, if both antibody and cAMP reagent were added within 30 seconds, there would be

minimum differences in measured final cAMP level. This discovery showed us that: if all other assay conditions were optimized, but timing of adding various cAMP reagent were not considered, we might get false increase or decrease of cAMP in both control and/or test compound group. This added another level of complexity for the cAMP assay. The same test also showed that the dilution effect of cAMP working solution (the volume of cAMP solution added in each well is 4 times that of antibody solution) are also minimized if adding antibody solution can be finished within 30 seconds. Ideally, the antibody should be added first and immediately followed by adding cAMP working solution within 30 seconds.

At this stage, another issue that might be affecting assay repeatability was discovered, which is how well the added antibody solution and cAMP working solution mixed with assay mixture. Through trial and error, we found that immediate shaking right after adding both antibody and cAMP working solution increased assay repeatability. This indicates that for viscous antibody solution and cAMP solution to execute its function for all wells equally and evenly, they must be thoroughly and evenly mixed with the assay mixture as soon as possible. Since the cAMP working solution is sensitive to light, a proper sized black plastic box was made to accommodate the glass microplate during the following shaking and 1-hour incubation step before the last reagent (solution A) was added.

5.2 Compound test

In the cAMP accumulation assay positive effect refers to a GABA-like effect, which means a further decrease of the measured cAMP signal, while a negative effect reverses the effect of GABA and increases the cAMP signal. Most compounds tested showed a certain level of effect on cAMP level. Test on GABA_B-R cell line shows, in the presence of GABA, compounds RB-490, RB-481, RB-482, and RB-475 increased the cAMP level (**figure 15**). RB-490 displayed the highest increase in cAMP signal. Additionally, compounds RB-476, RB-477 and TI400 all displayed a significant decrease in cAMP signal. RB-476 showed the same impact on the signal as RB-477, but with a lower compound concentration indicating that the compound has a stronger effect.

In the absence of GABA, referred to as forskolin-only or FSK-only seen on **figure 16**, compound RB-477 increased the signal and TI400 decreased the signal. This indicates that both compounds have some intrinsic effect on the cells, whether through the GABA_B-R specifically or by another cellular functions.

A consecutive test on wild-type cells was conducted to find out whether the activity we've seen with the compounds were specific to the GABA_B-R or not. In this assay, the compounds RB-492, RB-481, and RB-477 increased the signal, while RB-480 and TI400 slightly decreased the signal. Since the test on wild type were performed only once, more repeats of the test are needed to draw a proper conclusion.

To summarize: compound RB-490, RB-482, and RB-475 showed a GABA_B-R NAM-like effect by increasing the signal only in the presence of GABA; and compound RB-476 showed a GABA_B-R PAM-like effect by decreasing the signal only in the presence of GABA. Compound RB-491 and RB-478 had no effect in any of the tests, RB-492 and RB-480 only have effect on wild-type cells. And RB-477 has opposing effects in presence and absence of GABA. This suggests that RB-477 most likely also is a PAM, however it is not specific to GABA_B-R. Interestingly, compound RB-492 and RB-480 only possess effect on wild-type cell lines, which indicates its binding to alternative target. . The most promising compounds tested in the cAMP accumulation assay was the two compounds TI400 and RB-490, shown on **figure 18**.

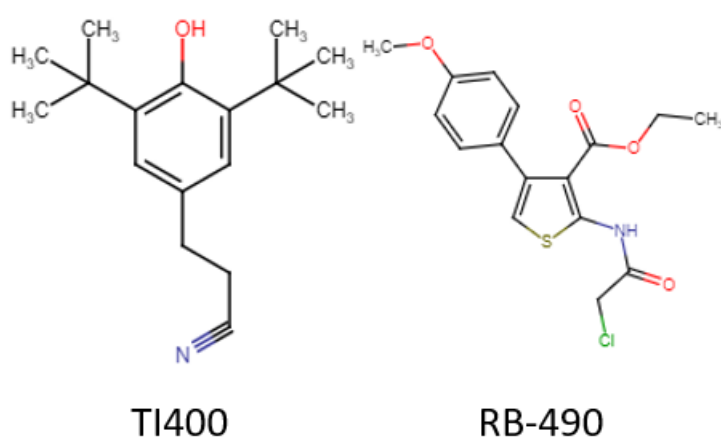


Figure 18: Structures of appealing candidates TI400 and RB-490.

TI400 was a previous hit which has been tested within the research group prior to this thesis. The results for TI400 confirmed what had already been reported: the feature of an ago-PAM (Inducing its own intrinsic effect like an agonist at the absence of GABA). The main structure bare resemblance to CLH304a, a known allosteric modulator. RB-490 is one of the new possible hits and portrays a NAM-like pattern in cAMP accumulation assay by increasing the signal only at the presence of GABA. Evidently, the RB-compounds described in this thesis are all very similar to each other and contain a combination of alterations on each carbon of the

main thiophene ring structure containing sulphur. All these compounds share an amido-group as well from the 2nd carbon, but with slight alterations between some compounds as well. **Figure 10** shown in the methods section depicts these alterations. RB-490 specifically, has a methoxybenzene on its 4th carbon and a 2-chloroacetamido on the 2nd carbon.

Other compounds (see appendix B) with the same 2-chloroacetamido group, such as RB-482, and RB-475 (with the exception of RB-480) also portray a NAM-like effect. This suggest an importance associated with this chemical group. Other alterations, such as the butamido- and 4-chlorobutamido groups, produced a variety of effects. Interestingly, RB-477, RB-476, and RB-482 all share an ethyl group on the 4th carbon of the thiophene ring, and all share unique activity in the presence of GABA. However, RB-477 has an opposing effect in the absence of GABA.

Due to limited time, we only did a test run of radioligand binding assay which yielded inconclusive results. However, the successful finishing of filtration steps gave future optimization of the assay a solid foundation. In theory, the cAMP accumulation assay alone is not enough to give conclusive evidence that a given compound is an allosteric binder. Therefore, an optimized radioligand binding assay in the future would be essential to clarify the compound candidate suggested from cAMP assay.

6 Conclusion

To establish a functional assay for GABA_B-R modulator screening could be challenging. Oftentimes, different lab does not have the same instruments used in assay protocols either from literature or reagent manufacturer's product data sheet. Therefore, modifying the assay protocol to fit local lab condition is a common practice. In our lab, we utilized a cAMP assay that is run in a water bath by using in-house built glass microplate. These helped to overcome issues like microplate edge effect, temperature fluctuation and reaction speed control. In addition to other minor adjustment in assay procedure, a functional assay protocol that produce a repeatable result was fully established.

With this protocol, commercial CHO-K1 cell line containing GABA_B-R was used to test various compounds in the presence and absence of GABA. We found several compounds have effects resemble allosteric modulators. Compounds RB-490, RB-482, and RB-475 have a NAM-like effect. Compounds RB-476, RB-477, and TI400 have PAM-like effect.

7 Further prospects

First and foremost, the radioligand binding assay should be conducted for all compounds, including those assumed to be ineffective. This might detect the effect of SAMs, weak PAM-antagonists, or ago-NAMs. Additionally, more repeated test might be needed for compound RB-490, RB-475, RB-482, RB-476, TI400, and RB-477. And lastly, although the cAMP accumulation assay is fully functional in its present state, a further optimization might be needed. Such as, designing an antibody preloading system to reduce the time for adding antibody solution and cAMP working solution from 30 seconds to within 10 seconds.

8 References

1. Ludwig PE, Reddy V, Varacallo M. Neuroanatomy, Central Nervous System (CNS). In: StatPearls [Internet]. Treasure Island (FL); 2020. Available from: <https://www.ncbi.nlm.nih.gov/pubmed/28723039>
2. Konan LM, Reddy V, Mesfin FB. Neuroanatomy, Cerebral Blood Supply. In: StatPearls [Internet]. Treasure Island (FL); 2020. Available from: <https://www.ncbi.nlm.nih.gov/pubmed/30335330>
3. Hall JE. Guyton and Hall textbook of medical physiology. 2016.
4. J. Gordon Betts James A. Wise, Eddie Johnson, Brandon Poe, Dean H. Kruse, Oksana Korol, Jody E. Johnson, Mark Womble, Peter DeSaix KAY. Anatomy & Physiology. 2013;Chapter 12-13. Available from: <https://openstax.org/books/anatomy-and-physiology/pages/12-introduction>
5. Thau L, Reddy V, Singh P. Anatomy, Central Nervous System. In: StatPearls [Internet]. Treasure Island (FL); 2020. Available from: <https://www.ncbi.nlm.nih.gov/pubmed/31194336>
6. Evenseth LSM, Ocello R, Gabrielsen M, Masetti M, Recanatini M, Sylte I, et al. Exploring Conformational Dynamics of the Extracellular Venus flytrap Domain of the GABAB Receptor: A Path-Metadynamics Study. J Chem Inf Model [Internet]. 2020/04/03. 2020;60(4):2294–303. Available from: <https://www.ncbi.nlm.nih.gov/pubmed/32233432>
7. Evenseth LSM. Ligand binding and dynamics of the GABAB receptor Venus flytrap domain [Internet]. Tromsø: UiT The Arctic University of Norway; 2019. Available from: <https://munin.uit.no/handle/10037/17041>
8. Barnett MW, Larkman PM. The action potential. Pr Neurol [Internet]. 2007/05/23. 2007;7(3):192–7. Available from: <https://www.ncbi.nlm.nih.gov/pubmed/17515599>
9. Katritch V, Cherezov V, Stevens RC. Structure-Function of the G Protein–Coupled Receptor Superfamily. Annu Rev Pharmacol Toxicol [Internet]. 2013;53(1):531–56. Available from: <https://www.annualreviews.org/doi/abs/10.1146/annurev-pharmtox-032112-135923>

10. Fredriksson R, Lagerström MC, Lundin L-G, Schiöth HB. The G-Protein-Coupled Receptors in the Human Genome Form Five Main Families. Phylogenetic Analysis, Paralogon Groups, and Fingerprints. *Mol Pharmacol* [Internet]. 2003;63(6):1256–72. Available from:
<https://molpharm.aspetjournals.org/content/molpharm/63/6/1256.full.pdf>
11. Munk C, Isberg V, Mordalski S, Harpsøe K, Rataj K, Hauser AS, et al. GPCRdb: the G protein-coupled receptor database – an introduction. *Br J Pharmacol* [Internet]. 2016;173(14):2195–207. Available from:
<https://bpspubs.onlinelibrary.wiley.com/doi/abs/10.1111/bph.13509>
12. Sutkeviciute I, Vilardaga JP. Structural insights into emergent signaling modes of G protein-coupled receptors. *J Biol Chem* [Internet]. 2020/06/24. 2020;295(33):11626–42. Available from: <https://www.ncbi.nlm.nih.gov/pubmed/32571882>
13. Neves SR, Ram PT, Iyengar R. G Protein Pathways. *Science* (80-) [Internet]. 2002;296(5573):1636–9. Available from:
<https://science.sciencemag.org/content/sci/296/5573/1636.full.pdf>
14. Frangaj A, Fan QR. Structural biology of GABAB receptor. *Neuropharmacology* [Internet]. 2017/10/17. 2018;136(Pt A):68–79. Available from:
<https://www.ncbi.nlm.nih.gov/pubmed/29031577>
15. Hilger D, Masureel M, Kobilka BK. Structure and dynamics of GPCR signaling complexes. *Nat Struct Mol Biol* [Internet]. 2018/01/13. 2018;25(1):4–12. Available from: <https://www.ncbi.nlm.nih.gov/pubmed/29323277>
16. Syrovatkina V, Alegre KO, Dey R, Huang XY. Regulation, Signaling, and Physiological Functions of G-Proteins. *J Mol Biol* [Internet]. 2016/08/16. 2016;428(19):3850–68. Available from:
<https://www.ncbi.nlm.nih.gov/pubmed/27515397>
17. Siehler S. Regulation of RhoGEF proteins by G12/13-coupled receptors. *Br J Pharmacol* [Internet]. 2009/02/20. 2009;158(1):41–9. Available from:
<https://www.ncbi.nlm.nih.gov/pubmed/19226283>
18. Gurevich V V, Gurevich E V. Arrestins: Critical Players in Trafficking of Many

- GPCRs. *Prog Mol Biol Transl Sci* [Internet]. 2015/06/10. 2015;132:1–14. Available from: <https://www.ncbi.nlm.nih.gov/pubmed/26055052>
19. Chun L, Zhang WH, Liu JF. Structure and ligand recognition of class C GPCRs. *Acta Pharmacol Sin* [Internet]. 2012/01/31. 2012;33(3):312–23. Available from: <https://www.ncbi.nlm.nih.gov/pubmed/22286915>
 20. Pin JP, Galvez T, Prezeau L. Evolution, structure, and activation mechanism of family 3/C G-protein-coupled receptors. *Pharmacol Ther* [Internet]. 2003/06/05. 2003;98(3):325–54. Available from: <https://www.ncbi.nlm.nih.gov/pubmed/12782243>
 21. Rondard P, Liu J, Huang S, Malhaire F, Vol C, Pinault A, et al. Coupling of agonist binding to effector domain activation in metabotropic glutamate-like receptors. *J Biol Chem* [Internet]. 2006/06/22. 2006;281(34):24653–61. Available from: <https://www.ncbi.nlm.nih.gov/pubmed/16787923>
 22. Kantamneni S. Modulation of Neurotransmission by the GABAB Receptor. In: Colombo G, editor. *GABAB Receptor* [Internet]. Cham: Springer International Publishing; 2016. p. 109–28. Available from: https://doi.org/10.1007/978-3-319-46044-4_7
 23. Bormann J. The ‘ABC’ of GABA receptors. *Trends Pharmacol Sci* [Internet]. 2000;21(1):16–9. Available from: <https://www.sciencedirect.com/science/article/pii/S0165614799014133>
 24. Castelli MP, Gessa GL. Distribution and Localization of the GABAB Receptor. In: Colombo G, editor. *GABAB Receptor* [Internet]. Cham: Springer International Publishing; 2016. p. 75–92. Available from: https://doi.org/10.1007/978-3-319-46044-4_5
 25. Evenseth LSM, Gabrielsen M, Sylte I. The GABAB Receptor-Structure, Ligand Binding and Drug Development. *Molecules* [Internet]. 2020/07/11. 2020;25(13). Available from: <https://www.ncbi.nlm.nih.gov/pubmed/32646032>
 26. Urwyler S. Allosteric Modulators: The New Generation of GABAB Receptor Ligands. In: Colombo G, editor. *GABAB Receptor* [Internet]. Cham: Springer International Publishing; 2016. p. 357–75. Available from: <https://doi.org/10.1007/978-3-319->

27. Porcu A, Mostallino R, Serra V, Melis M, Sogos V, Beggiato S, et al. COR758, a negative allosteric modulator of GABAB receptors. *Neuropharmacology* [Internet]. 2021;189:108537. Available from: <https://www.sciencedirect.com/science/article/pii/S0028390821000915>
28. Rose TR, Wickman K. Mechanisms and Regulation of Neuronal GABAB Receptor-Dependent Signaling. In Berlin, Heidelberg: Springer Berlin Heidelberg; p. 1–41. Available from: https://doi.org/10.1007/7854_2020_129
29. Luján R, Aguado C. Chapter Five - Localization and Targeting of GIRK Channels in Mammalian Central Neurons. In: Slesinger PA, Wickman KBT-IR of N, editors. *Structure to Function of G Protein-Gated Inwardly Rectifying (GIRK) Channels* [Internet]. Academic Press; 2015. p. 161–200. Available from: <https://www.sciencedirect.com/science/article/pii/S0074774215000252>
30. Proft J, Weiss N. G protein regulation of neuronal calcium channels: back to the future. *Mol Pharmacol*. 2015 Jun;87(6):890–906.
31. Chalifoux JR, Carter AG. GABAB receptor modulation of synaptic function. *Curr Opin Neurobiol* [Internet]. 2011/03/08. 2011;21(2):339–44. Available from: <https://www.ncbi.nlm.nih.gov/pubmed/21376567>
32. Bettler B, Kaupmann K, Mosbacher J, Gassmann M. Molecular structure and physiological functions of GABA(B) receptors. *Physiol Rev* [Internet]. 2004/07/23. 2004;84(3):835–67. Available from: <https://www.ncbi.nlm.nih.gov/pubmed/15269338>
33. Calver AR, Medhurst AD, Robbins MJ, Charles KJ, Evans ML, Harrison DC, et al. The expression of GABA(B1) and GABA(B2) receptor subunits in the cNS differs from that in peripheral tissues. *Neuroscience* [Internet]. 2000/09/21. 2000;100(1):155–70. Available from: <https://www.ncbi.nlm.nih.gov/pubmed/10996466>
34. Castelli MP, Ingianni A, Stefanini E, Gessa GL. Distribution of GABA(B) receptor mRNAs in the rat brain and peripheral organs. *Life Sci* [Internet]. 1999/05/05. 1999;64(15):1321–8. Available from: <https://www.ncbi.nlm.nih.gov/pubmed/10227588>

35. Isomoto S, Kaibara M, Sakurai-Yamashita Y, Nagayama Y, Uezono Y, Yano K, et al. Cloning and tissue distribution of novel splice variants of the rat GABAB receptor. *Biochem Biophys Res Commun* [Internet]. 1999/01/06. 1998;253(1):10–5. Available from: <https://www.ncbi.nlm.nih.gov/pubmed/9875211>
36. Pfaff T, Malitschek B, Kaupmann K, Prezeau L, Pin JP, Bettler B, et al. Alternative splicing generates a novel isoform of the rat metabotropic GABA(B)R1 receptor. *Eur J Neurosci* [Internet]. 1999/08/24. 1999;11(8):2874–82. Available from: <https://www.ncbi.nlm.nih.gov/pubmed/10457184>
37. Xu C, Zhang W, Rondard P, Pin JP, Liu J. Complex GABAB receptor complexes: how to generate multiple functionally distinct units from a single receptor. *Front Pharmacol* [Internet]. 2014/02/28. 2014;5:12. Available from: <https://www.ncbi.nlm.nih.gov/pubmed/24575041>
38. Lorente P, Lacampagne A, Pouzeratte Y, Richards S, Malitschek B, Kuhn R, et al. gamma-aminobutyric acid type B receptors are expressed and functional in mammalian cardiomyocytes. *Proc Natl Acad Sci U S A* [Internet]. 2000/07/19. 2000;97(15):8664–9. Available from: <https://www.ncbi.nlm.nih.gov/pubmed/10900022>
39. Magnaghi V, Ballabio M, Consoli A, Lambert JJ, Roglio I, Melcangi RC. GABA receptor-mediated effects in the peripheral nervous system: A cross-interaction with neuroactive steroids. *J Mol Neurosci* [Internet]. 2006/04/25. 2006;28(1):89–102. Available from: <https://www.ncbi.nlm.nih.gov/pubmed/16632878>
40. Pilc A, Nowak G. GABAergic hypotheses of anxiety and depression: focus on GABA-B receptors. *Drugs Today (Barc)*. 2005 Nov;41(11):755–66.
41. Tyacke RJ, Lingford-Hughes A, Reed LJ, Nutt DJ. GABAB receptors in addiction and its treatment. *Adv Pharmacol*. 2010;58:373–96.
42. Fatemi SH, Folsom TD, Thuras PD. GABA(A) and GABA(B) receptor dysregulation in superior frontal cortex of subjects with schizophrenia and bipolar disorder. *Synapse*. 2017 Jul;71(7).
43. Maffioletti E, Minelli A, Tardito D, Gennarelli M. Blues in the Brain and Beyond: Molecular Bases of Major Depressive Disorder and Relative Pharmacological and

- Non-Pharmacological Treatments. *Genes (Basel)* [Internet]. 2020 Sep 18;11(9):1089. Available from: <https://pubmed.ncbi.nlm.nih.gov/32961910>
44. Vergas R. The GABAergic System: An Overview of Physiology, Physiopathology and Therapeutics. *Int J Clin Pharmacol Pharmacother* [Internet]. 2018;3(142):9. Available from: <https://www.graphyonline.com/archives/IJCPP/2018/IJCPP-142/#headerCitation>
 45. Brown KM, Roy KK, Hockerman GH, Doerksen RJ, Colby DA. Activation of the γ -Aminobutyric Acid Type B (GABA(B)) Receptor by Agonists and Positive Allosteric Modulators. *J Med Chem* [Internet]. 2015/04/24. 2015 Aug 27;58(16):6336–47. Available from: <https://pubmed.ncbi.nlm.nih.gov/25856547>
 46. Urwyler S, Mosbacher J, Lingenhoechl K, Heid J, Hofstetter K, Froestl W, et al. Positive allosteric modulation of native and recombinant gamma-aminobutyric acid(B) receptors by 2,6-Di-tert-butyl-4-(3-hydroxy-2,2-dimethyl-propyl)-phenol (CGP7930) and its aldehyde analog CGP13501. *Mol Pharmacol*. 2001 Nov;60(5):963–71.
 47. Mugnaini C, Pedani V, Casu A, Lobina C, Casti A, Maccioni P, et al. Synthesis and Pharmacological Characterization of 2-(Acylamino)thiophene Derivatives as Metabolically Stable, Orally Effective, Positive Allosteric Modulators of the GABAB Receptor. *J Med Chem* [Internet]. 2013 May 9;56(9):3620–35. Available from: <https://doi.org/10.1021/jm400144w>
 48. Gawdi R, Emmady PD. Physiology, Blood Brain Barrier. In: *StatPearls* [Internet]. Treasure Island (FL); 2020. Available from: <https://www.ncbi.nlm.nih.gov/pubmed/32491653>
 49. Pardridge WM. Drug transport across the blood-brain barrier. *J Cereb Blood Flow Metab* [Internet]. 2012/08/30. 2012;32(11):1959–72. Available from: <https://www.ncbi.nlm.nih.gov/pubmed/22929442>
 50. Monod J, Wyman J, Changeux JP. On the nature of allosteric transitions: A plausible model. *J Mol Biol*. 1965 May;12:88–118.
 51. Hall DA. Modeling the Functional Effects of Allosteric Modulators at Pharmacological Receptors: An Extension of the Two-State Model of Receptor Activation. *Mol Pharmacol* [Internet]. 2000 Dec 1;58(6):1412 LP – 1423. Available from:

<http://molpharm.aspetjournals.org/content/58/6/1412.abstract>

52. Wold EA, Chen J, Cunningham KA, Zhou J. Allosteric Modulation of Class A GPCRs: Targets, Agents, and Emerging Concepts. *J Med Chem* [Internet]. 2018/08/15. 2019;62(1):88–127. Available from: <https://www.ncbi.nlm.nih.gov/pubmed/30106578>
53. Foster DJ, Conn PJ. Allosteric Modulation of GPCRs: New Insights and Potential Utility for Treatment of Schizophrenia and Other CNS Disorders. *Neuron* [Internet]. 2017/05/05. 2017;94(3):431–46. Available from: <https://www.ncbi.nlm.nih.gov/pubmed/28472649>
54. van Westen GJ, Gaulton A, Overington JP. Chemical, target, and bioactive properties of allosteric modulation. *PLoS Comput Biol* [Internet]. 2014/04/05. 2014;10(4):e1003559. Available from: <https://www.ncbi.nlm.nih.gov/pubmed/24699297>
55. Wenthur CJ, Gentry PR, Mathews TP, Lindsley CW. Drugs for allosteric sites on receptors. *Annu Rev Pharmacol Toxicol* [Internet]. 2013/10/12. 2014;54:165–84. Available from: <https://www.ncbi.nlm.nih.gov/pubmed/24111540>
56. Urwyler S, Pozza MF, Lingenhoehl K, Mosbacher J, Lampert C, Froestl W, et al. N,N'-Dicyclopentyl-2-methylsulfanyl-5-nitro-pyrimidine-4,6-diamine (GS39783) and structurally related compounds: novel allosteric enhancers of gamma-aminobutyric acidB receptor function. *J Pharmacol Exp Ther*. 2003 Oct;307(1):322–30.
57. Chen L-H, Sun B, Zhang Y, Xu T-J, Xia Z-X, Liu J-F, et al. Discovery of a Negative Allosteric Modulator of GABAB Receptors. *ACS Med Chem Lett* [Internet]. 2014 Jul 10;5(7):742–7. Available from: <https://doi.org/10.1021/ml500162z>
58. Kenakin TP. Chapter 5 - Allosteric Drug Effects. In: Kenakin TPBT-P in DD and D (Second E, editor. Academic Press; 2017. p. 101–29. Available from: <https://www.sciencedirect.com/science/article/pii/B9780128037522000053>
59. Haas LT, Salazar S V, Smith LM, Zhao HR, Cox TO, Herber CS, et al. Silent Allosteric Modulation of mGluR5 Maintains Glutamate Signaling while Rescuing Alzheimer's Mouse Phenotypes. *Cell Rep* [Internet]. 2017;20(1):76–88. Available from: <https://www.sciencedirect.com/science/article/pii/S2211124717308203>

60. Grundmann M, Bender E, Schamberger J, Eitner F. Pharmacology of Free Fatty Acid Receptors and Their Allosteric Modulators. *Int J Mol Sci* [Internet]. 2021 Feb 10;22(4):1763. Available from: <https://pubmed.ncbi.nlm.nih.gov/33578942>
61. Schaeffer WI. Terminology associated with cell, tissue, and organ culture, molecular biology, and molecular genetics. Tissue Culture Association Terminology Committee. *Vitr Cell Dev Biol J Tissue Cult Assoc*. 1990 Jan;26(1):97–101.
62. Hartung T, Balls M, Bardouille C, Blanck O, Coecke S, Gstraunthaler G, et al. ECVAM Good Cell Culture Practice Task Force Report 1. *Altern to Lab Anim* [Internet]. 2002 Jul 1;30(4):407–14. Available from: <https://doi.org/10.1177/026119290203000404>
63. Coecke S, Balls M, Bowe G, Davis J, Gstraunthaler G, Hartung T, et al. Guidance on good cell culture practice. a report of the second ECVAM task force on good cell culture practice. *Altern Lab Anim*. 2005 Jun;33(3):261–87.
64. Pamies D, Bal-Price A, Simeonov A, Tagle D, Allen D, Gerhold D, et al. Good Cell Culture Practice for stem cells and stem-cell-derived models. *ALTEX*. 2017;34(1):95–132.
65. Fischer S, Handrick R, Otte K. The art of CHO cell engineering: A comprehensive retrospect and future perspectives. *Biotechnol Adv*. 2015 Dec;33(8):1878–96.
66. Wuest DM, Harcum SW, Lee KH. Genomics in mammalian cell culture bioprocessing. *Biotechnol Adv*. 2012;30(3):629–38.
67. Hill SJ, Williams C, May LT. Insights into GPCR pharmacology from the measurement of changes in intracellular cyclic AMP; advantages and pitfalls of differing methodologies. *Br J Pharmacol* [Internet]. 2010 Nov;161(6):1266–75. Available from: <https://pubmed.ncbi.nlm.nih.gov/21049583>
68. Williams C. cAMP detection methods in HTS: selecting the best from the rest. *Nat Rev Drug Discov* [Internet]. 2004;3(2):125–35. Available from: <https://doi.org/10.1038/nrd1306>
69. Kamenetsky M, Middelhaufe S, Bank EM, Levin LR, Buck J, Steegborn C. Molecular details of cAMP generation in mammalian cells: a tale of two systems. *J Mol Biol*

- [Internet]. 2006/07/28. 2006 Sep 29;362(4):623–39. Available from:
<https://pubmed.ncbi.nlm.nih.gov/16934836>
70. Hulme EC, Trevethick MA. Ligand binding assays at equilibrium: validation and interpretation. *Br J Pharmacol* [Internet]. 2010 Nov;161(6):1219–37. Available from:
<https://pubmed.ncbi.nlm.nih.gov/20132208>
71. Freyd T, Warszycki D, Mordalski S, Bojarski AJ, Sylte I, Gabrielsen M. Ligand-guided homology modelling of the GABAB2 subunit of the GABAB receptor. *PLoS One* [Internet]. 2017 Mar 21;12(3):e0173889. Available from:
<https://doi.org/10.1371/journal.pone.0173889>

9 Appendices

9.1 Appendix A

Cell culture and assay recipes

2xHBSS: 59.270mL dH₂O + 730μL 1M NaOH + 10mL of each stock (Stock 1-4)

Stock 1: 5160mM/L NaCl + 400mM/L D-glucose + 200mM/L KCl

Stock 2: 52mM/L CaCl₂

Stock 3: 40mM/L MgCl₂

Stock 4: 400mM/L 4-(2-hydroxyethyl)-1-piperazineethanesulfonic acid HEPES

5G: 37.2mL dH₂O + 800μL 1M NaOH + 2mL 100mM D-glucose

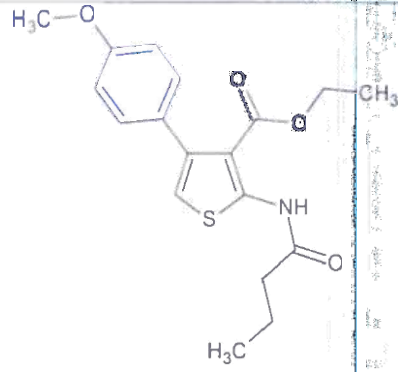
Radioligand assay buffer: 40mM Tris-HCl + 236mM NaCl + 9.4mM KCl + 4mM CaCl₂ + 2.4mM KH₂PO₄ + 2.4mM MgSO₄ + 10mM D-glucose, combined in 200mL dH₂O set to pH=7.43 at 23.7°C

Radioligand wash buffer: 50mM Tris-HCl + 2.5mM CaCl₂, combined in 1 litre dH₂O set to pH=7.36 at 24.4°C

9.2 Appendix B

Test compounds from the Polish Academy of Sciences

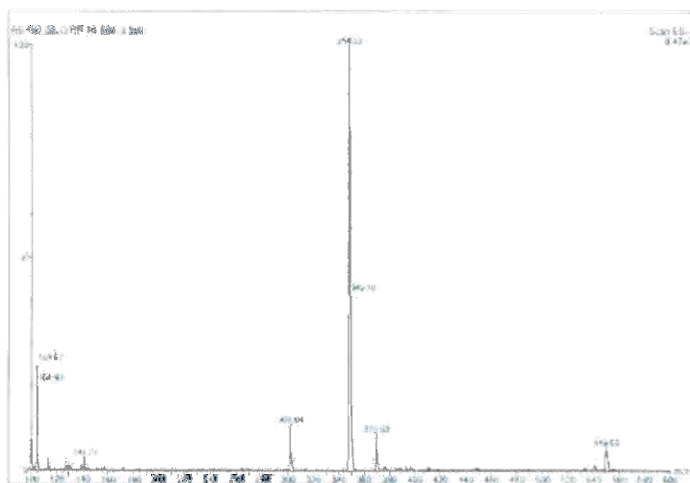
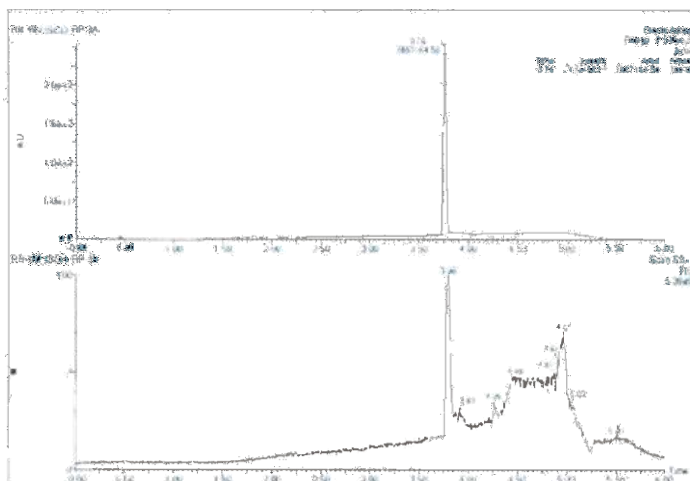
The following pages contain a list of the new hits test compounds investigated in this thesis. The compounds were provided to us through our collaborators Andrzej J. Bojarski and his research group in Krakow, Poland at the Polish Academy of Sciences. The compounds is listed in the exact format he sent to our group.

Name:	RB-492 (analog Comps 9 and 11)	
Molecular formula:	C ₁₈ H ₂₁ NO ₄ S	
Formula weight	347.429	
Amount:	63 mg	
Form:	White, solid	
Identification:	LCMS, ¹ H NMR, ¹³ C NMR	

¹H NMR (500 MHz, DMSO-*d*₆) δ 10.96 (s, 1H), 7.24 – 7.17 (m, 2H), 6.94 – 6.87 (m, 2H), 6.82 (d, *J* = 0.7 Hz, 1H), 4.08 (q, *J* = 7.1 Hz, 2H), 3.77 (s, 3H), 2.51 (t, *J* = 7.4 Hz, 2H), 1.65 (h, *J* = 7.4 Hz, 2H), 0.95 (dt, *J* = 20.0, 7.2 Hz, 6H).

¹³C NMR (126 MHz, DMSO-*d*₆) δ 170.29, 164.73, 158.40, 147.98, 138.63, 129.90, 129.37, 114.81, 112.90, 111.72, 60.21, 55.08, 37.52, 18.25, 13.50, 13.45.

LC-MS: R_T = 3.76 min (purity: 100%), *m/z* [M+H⁺] found: 348.0 (calc. 348.1).

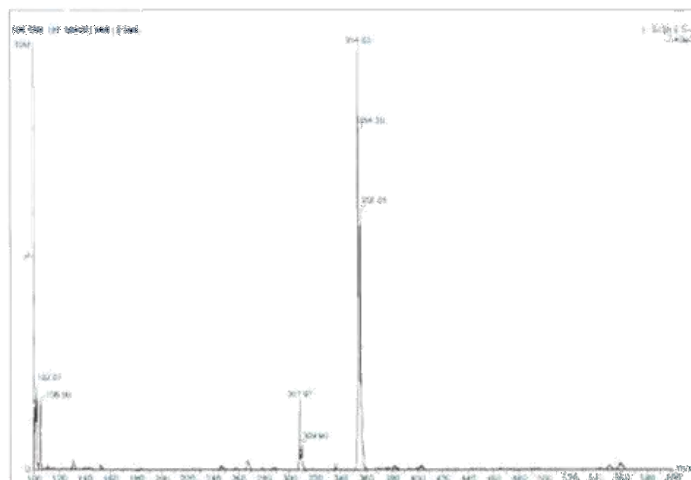
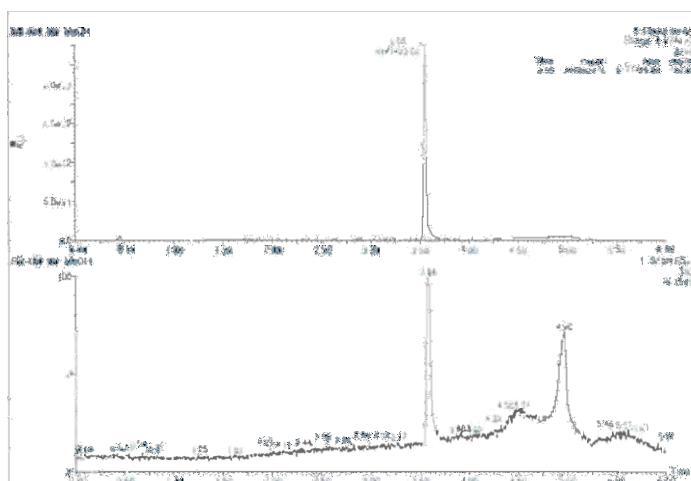


Name:	RB-490 (analog Comps 9 and 11)	
Molecular formula:	C ₁₆ H ₁₆ ClNO ₄ S	
Formula weight	353.820	
Amount:	123 mg	
Form:	Off white, solid	
Identification:	LCMS, ¹ H NMR, ¹³ C NMR	

¹H NMR (500 MHz, DMSO-*d*₆) δ 11.65 (s, 1H), 7.26 – 7.19 (m, 2H), 6.94 – 6.88 (m, 3H), 4.62 (s, 2H), 4.10 (q, *J* = 7.1 Hz, 2H), 3.77 (s, 3H), 0.97 (t, *J* = 7.1 Hz, 3H).

¹³C NMR (126 MHz, DMSO-*d*₆) δ 164.69, 164.39, 158.51, 147.30, 138.95, 130.02, 129.14, 115.65, 112.94, 112.77, 60.48, 55.12, 42.58, 13.52.

LC-MS: R_T = 3.55 min (purity: 100%), *m/z* [M+H⁺] found: 354.0 (calc. 354.0).

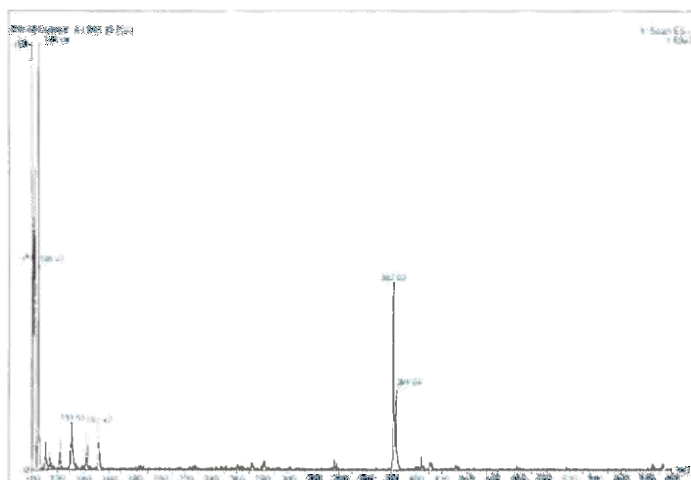
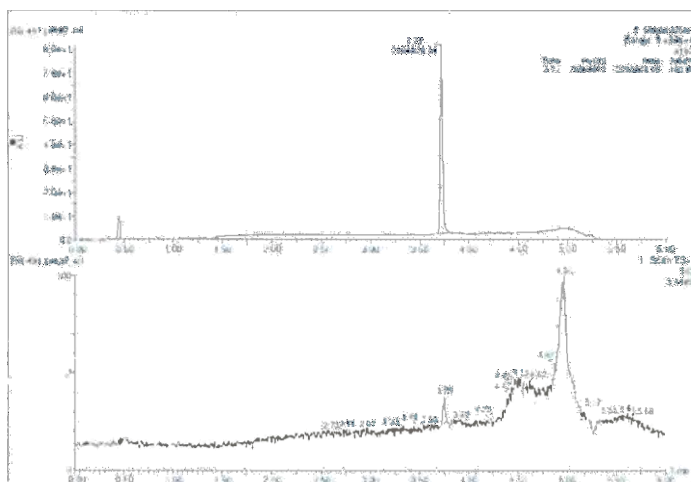


Name:	RB-491 (analog Comps 9 and 11)	
Molecular formula:	C ₁₈ H ₂₀ ClNO ₄ S	
Formula weight	381.874	
Amount:	73 mg	
Form:	Yellow, solid	
Identification:	LCMS, ¹ H NMR, ¹³ C NMR	

¹H NMR (500 MHz, DMSO-*d*₆) δ 10.98 (s, 1H), 7.24 – 7.17 (m, 2H), 6.94 – 6.87 (m, 2H), 6.84 (d, *J* = 0.7 Hz, 1H), 4.08 (q, *J* = 7.1 Hz, 2H), 3.77 (s, 3H), 3.71 (t, *J* = 6.6 Hz, 2H), 2.70 (t, *J* = 7.3 Hz, 2H), 2.08 (dq, *J* = 7.8, 6.7 Hz, 2H), 0.98 (t, *J* = 7.1 Hz, 3H).

¹³C NMR (126 MHz, DMSO-*d*₆) δ 169.54, 164.61, 158.42, 147.56, 138.63, 129.86, 129.29, 114.92, 112.95, 112.13, 60.25, 55.10, 44.62, 40.01, 39.84, 39.67, 39.51, 39.34, 39.17, 39.00, 32.84, 27.68, 13.53.

LC-MS: R_T = 3.72 min (purity: 100%), *m/z* [M+H⁺] found: 382.0 (calc. 382.1).

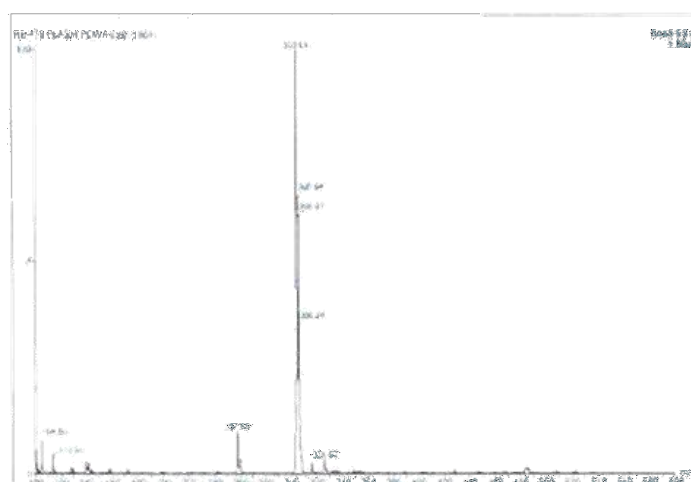
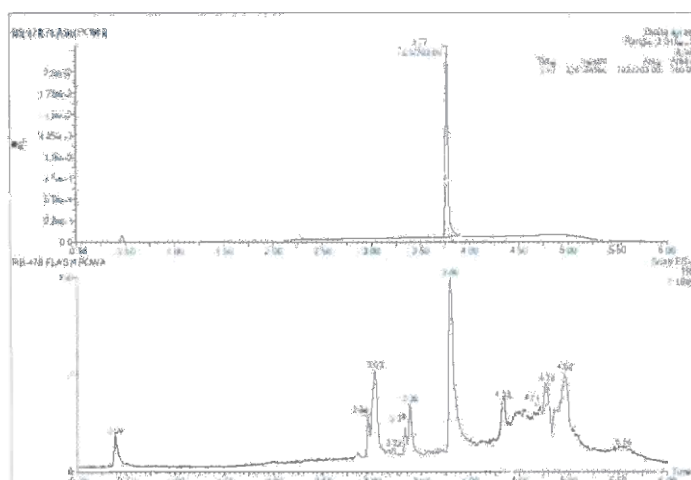


Name:	RB-478 (Compd 35)	
Molecular formula:	C ₁₃ H ₁₈ ClNO ₃ S	
Formula weight	303.805	
Amount:	503 mg	
Form:	Light beige, solid	
Identification:	LCMS, ¹ H NMR, ¹³ C NMR	

¹H NMR (500 MHz, DMSO-*d*₆) δ 10.95 (s, 1H), 4.28 (q, *J* = 7.1 Hz, 2H), 3.69 (t, *J* = 6.6 Hz, 2H), 2.64 (dd, *J* = 7.7, 7.0 Hz, 2H), 2.21 (s, 3H), 2.17 (s, 3H), 2.05 (dq, *J* = 7.8, 6.7 Hz, 2H), 1.32 (t, *J* = 7.1 Hz, 3H).

¹³C NMR (126 MHz, DMSO-*d*₆) δ 168.95, 164.94, 144.91, 128.44, 122.79, 112.55, 60.40, 44.59, 32.88, 27.71, 14.02, 13.92, 11.96.

LC-MS: R_T = 3.77 min (purity: 100%), *m/z* [M+H⁺] found: 303.6 (calc. 304.1).

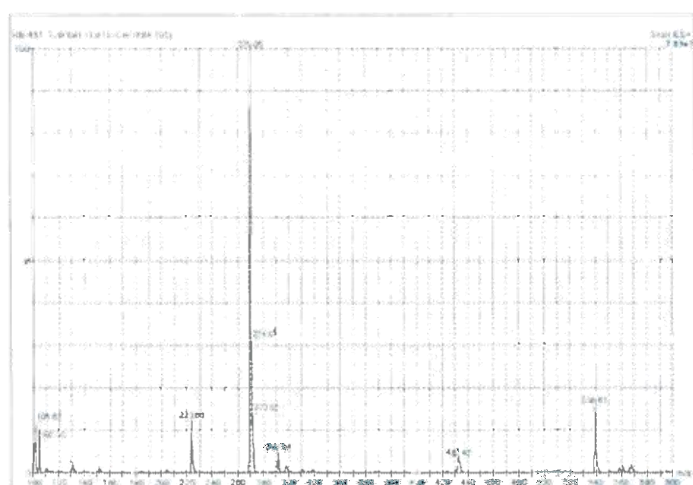
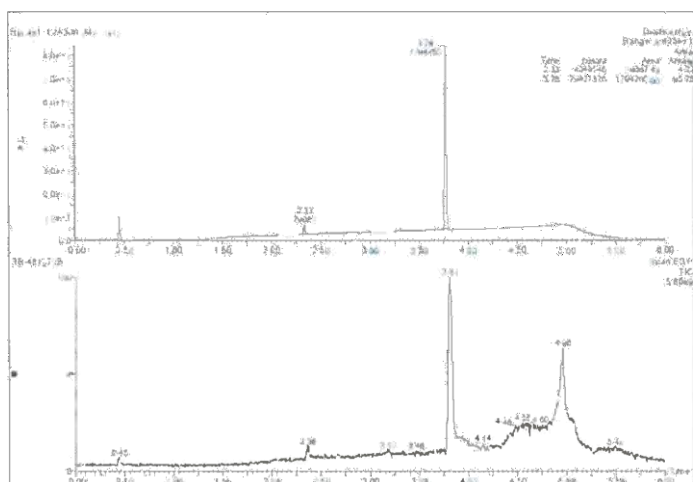


Name:	RB-481 (analog Compd 35)	
Molecular formula:	C ₁₃ H ₁₉ NO ₃ S	
Formula weight	269.360	
Amount:	192 mg	
Form:	Pale yellow, oil	
Identification:	LCMS, ¹ H NMR, ¹³ C NMR	

¹H NMR (500 MHz, DMSO-*d*₆) δ 10.94 (s, 1H), 4.29 (q, *J* = 7.1 Hz, 2H), 2.46 (t, *J* = 7.4 Hz, 2H), 2.21 (s, 3H), 2.18 (s, 3H), 1.62 (h, *J* = 7.4 Hz, 2H), 1.32 (t, *J* = 7.1 Hz, 3H), 0.91 (t, *J* = 7.4 Hz, 3H).

¹³C NMR (126 MHz, DMSO-*d*₆) δ 169.72, 165.05, 145.19, 128.38, 122.64, 112.27, 60.39, 37.56, 18.25, 14.02, 13.95, 13.45, 11.95.

LC-MS: R_T = 3.78 min (purity: 96%), *m/z* [M+H⁺] found: 269.6 (calc. 270.0).

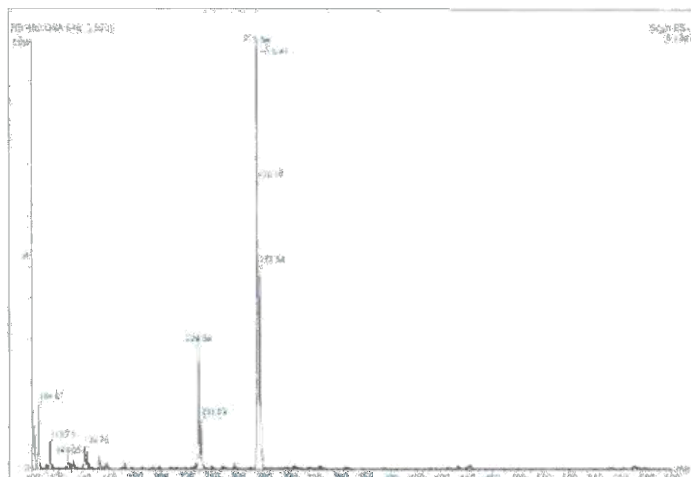
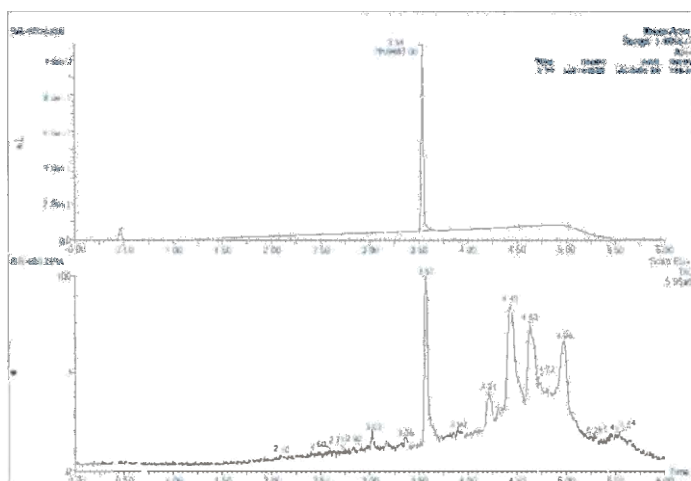


Name:	RB-480 (analog Compd 35)	
Molecular formula:	C ₁₁ H ₁₄ ClNO ₃ S	
Formula weight	275.752	
Amount:	712 mg	
Form:	Off white, solid	
Identification:	LCMS, ¹ H NMR, ¹³ C NMR	

¹H NMR (500 MHz, DMSO-*d*₆) δ 11.63 (s, 1H), 4.57 (s, 2H), 4.31 (q, *J* = 7.1 Hz, 2H), 2.24 (d, *J* = 0.8 Hz, 3H), 2.20 (d, *J* = 0.9 Hz, 3H), 1.33 (t, *J* = 7.1 Hz, 3H).

¹³C NMR (126 MHz, DMSO-*d*₆) δ 164.96, 163.82, 144.12, 128.89, 123.70, 113.47, 60.68, 42.55, 14.05, 13.95, 12.02.

LC-MS: R_T = 3.54 min (purity: 100%), *m/z* [M+H⁺] found: 275.6 (calc. 276.0).

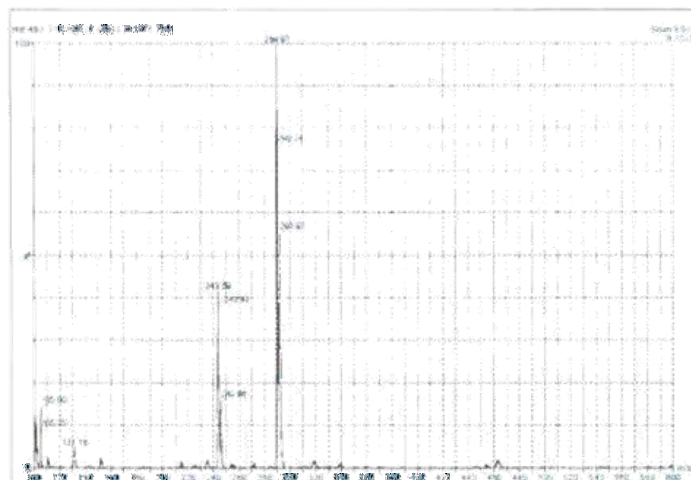
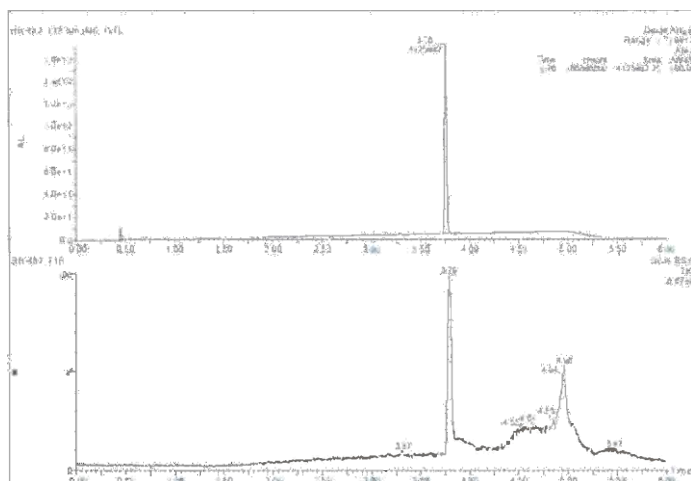


Name:	RB-482 (Compd 11)	
Molecular formula:	C ₁₂ H ₁₆ ClNO ₃ S	
Formula weight	289.778	
Amount:	271 mg	
Form:	White, solid	
Identification:	LCMS, ¹ H NMR, ¹³ C NMR	

¹H NMR (500 MHz, DMSO-*d*₆) δ 11.64 (s, 1H), 4.57 (s, 2H), 4.32 (q, *J* = 7.1 Hz, 2H), 2.67 (q, *J* = 7.6 Hz, 2H), 2.22 (s, 3H), 1.33 (t, *J* = 7.1 Hz, 3H), 1.14 (t, *J* = 7.5 Hz, 3H).

¹³C NMR (126 MHz, DMSO-*d*₆) δ 165.02, 163.81, 144.24, 131.01, 128.11, 113.59, 60.66, 42.55, 19.95, 15.61, 14.04, 13.76.

LC-MS: R_T = 3.76 min (purity: 100%), *m/z* [M+H⁺] found: 290.0 (calc. 290.0).

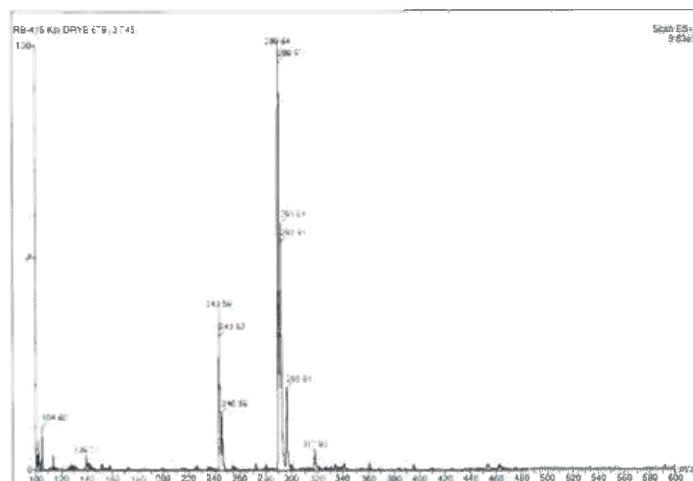
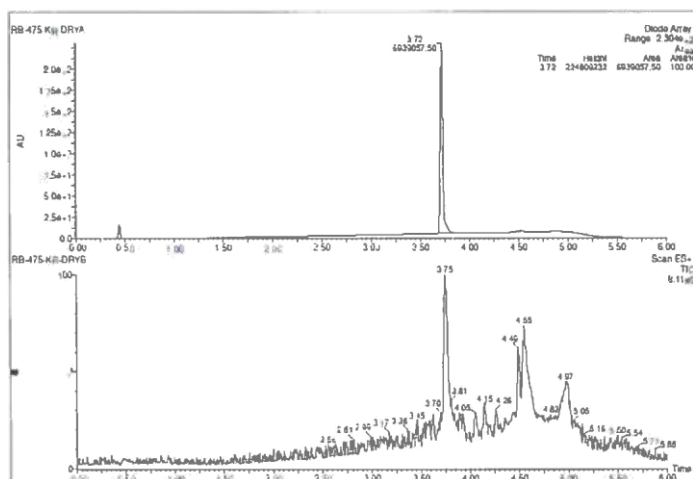


Name:	RB-475 (Compd 36)	
Molecular formula:	C ₁₂ H ₁₆ ClNO ₃ S	
Formula weight	289.778	
Amount:	500 mg	
Form:	White, solid	
Identification:	LCMS, ¹ H NMR, ¹³ C NMR	

¹H NMR (500 MHz, DMSO-*d*₆) δ 11.66 (s, 1H), 4.57 (s, 2H), 4.33 (q, *J* = 7.1 Hz, 2H), 2.71 (q, *J* = 7.3 Hz, 2H), 2.25 (s, 3H), 1.33 (t, *J* = 7.1 Hz, 3H), 1.03 (t, *J* = 7.4 Hz, 3H).

¹³C NMR (126 MHz, DMSO-*d*₆) δ 164.79, 163.82, 144.39, 135.36, 123.65, 112.75, 60.69, 42.55, 20.56, 14.78, 13.91, 11.65.

LC-MS: R_T = 3.72 min (purity: 100%), *m/z* [M+H⁺] found: 289.6 (calc. 290.0).

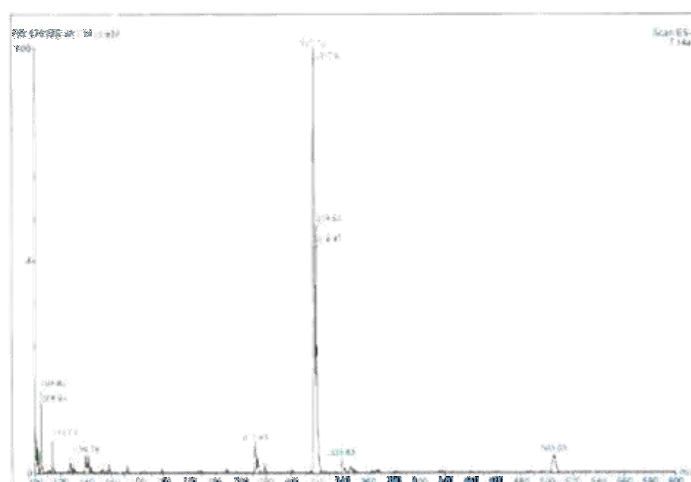
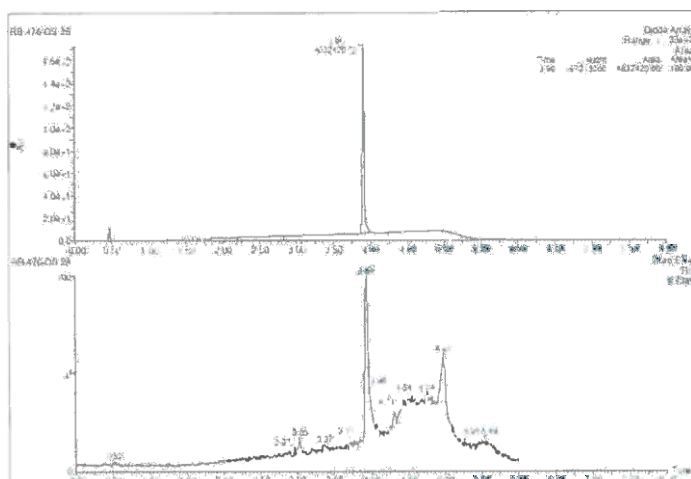


Name:	RB-476 (analog Compd 36)	
Molecular formula:	C ₁₄ H ₂₀ ClNO ₃ S	
Formula weight	317.831	
Amount:	308 mg	
Form:	Light yellow, solid	
Identification:	LCMS, ¹ H NMR, ¹³ C NMR	

¹H NMR (500 MHz, DMSO-*d*₆) δ 10.97 (s, 1H), 4.30 (q, *J* = 7.1 Hz, 2H), 3.68 (t, *J* = 6.6 Hz, 2H), 2.73 – 2.60 (m, 4H), 2.23 (s, 3H), 2.05 (dq, *J* = 7.8, 6.7 Hz, 2H), 1.32 (t, *J* = 7.1 Hz, 3H), 1.02 (t, *J* = 7.4 Hz, 3H).

¹³C NMR (125 MHz, DMSO-*d*₆) δ 172.00, 167.03, 151.75, 143.75, 123.92, 111.39, 60.88, 43.49, 33.67, 27.88, 20.62, 14.81, 14.23, 13.55.

LC-MS: R_T = 3.90 min (purity: 100%), *m/z* [M+H⁺] found: 317.7 (calc. 318.1).



Name:	RB-477 (Compd 38)	
Molecular formula:	C ₁₄ H ₂₁ NO ₃ S	
Formula weight	283.386	
Amount:	280 mg	
Form:	Light yellow, solid	
Identification:	LCMS, ¹ H NMR, ¹³ C NMR	

¹H NMR (500 MHz, DMSO-*d*₆) δ 10.96 (s, 1H), 4.30 (q, *J* = 7.1 Hz, 2H), 2.68 (q, *J* = 7.4 Hz, 2H), 2.45 (t, *J* = 7.4 Hz, 2H), 2.22 (s, 3H), 1.62 (h, *J* = 7.4 Hz, 2H), 1.32 (t, *J* = 7.1 Hz, 3H), 1.02 (t, *J* = 7.4 Hz, 3H), 0.91 (t, *J* = 7.4 Hz, 3H).

¹³C NMR (126 MHz, DMSO-*d*₆) δ 169.70, 164.87, 145.41, 134.89, 122.58, 111.54, 60.40, 37.59, 20.53, 18.27, 14.83, 13.88, 13.44, 11.58.

LC-MS: R_T = 3.94 min (purity: 100%), *m/z* [M+H⁺] found: 284.0 (calc. 284.1).

